



National Defence
Research and
Development Branch

Défense nationale
Bureau de recherche
et développement

TECHNICAL MEMORANDUM 96/229

Volume I

July 1996

MEASUREMENT AND LINEAR PREDICTION OF
HULL PRESSURE SPECTRA ON CFAV QUEST
— RESULTS OF Q210 —
Volume I

David C. Stredulinsky
Neil G. Pegg — Layton E. Gilroy

DISTRIBUTION STATEMENT A

Approved for public release
Distribution Unlimited

DTIC QUALITY INSPECTED 4

**Defence
Research
Establishment
Atlantic**



**Centre de
Recherches pour la
Défense
Atlantique**

Canada

19961016 066

DEFENCE RESEARCH ESTABLISHMENT ATLANTIC

9 GROVE STREET

P.O. BOX 1012
DARTMOUTH, N.S.
B2Y 3Z7

TELEPHONE
(902) 426-3100

CENTRE DE RECHERCHES POUR LA DÉFENSE ATLANTIQUE

9 GROVE STREET

C.P. BOX 1012
DARTMOUTH, N.É.
B2Y 3Z7



National Defence
Research and
Development Branch

Défense nationale
Bureau de recherche
et développement


MEASUREMENT AND LINEAR PREDICTION OF
HULL PRESSURE SPECTRA ON CFAV QUEST
— RESULTS OF Q210 —
Volume I

David C. Stredulinsky
Neil G. Pegg — Layton E. Gilroy

July 1996

Approved by C.W. Bright
Deputy Director General

Distribution Approved by C.W. Bright


For Deputy Director General

TECHNICAL MEMORANDUM 96/229 Volume I

**Defence
Research
Establishment
Atlantic**



**Centre de
Recherches pour la
Défense
Atlantique**

Canada

Abstract

Trial Q210 was undertaken in November 1993 on CFAV QUEST to measure hull pressure loads and structural response during various operational conditions in moderate seas. This memorandum describes results of measurements and predictions for ship motions and for the pressure loads; results for the strain measurements and predictions will be discussed in a later report. Pressure spectra derived from the measurements are compared to predictions from PRECAL, a three-dimensional linear ship motion and load prediction code. The measured and predicted pressure spectra show reasonable agreement, indicating the strong potential of using PRECAL to predict fatigue load histories for ship hull structures.

This report is presented in two volumes with Volume I containing the main body and Volume II containing the Appendices. Volume I will be given full distribution with Volume II being distributed only on request.

Résumé

Trial Q210 a été embarqué à bord du CFAV QUEST en novembre 1993 pour mesurer les efforts de pression sur la carène et la réponse de la structure dans des conditions de mer linéaire variées. Cette note décrit les résultats des mesures et les prédictions effectuées concernant les efforts de pression; on discutera des résultats des mesures des efforts et de leur prédiction dans un prochain rapport. On compare les spectres de pression obtenus à partir des mesures à ceux prédits par PRECAL, un code de calcul des chargements et des mouvements d'un navire en théorie linéaire tridimensionnelle. Les spectres de pressions mesurés et prédits s'accordent raisonnablement bien et ceci indique le grand intérêt d'utiliser PRECAL pour prédire pour les structures des carènes des navires les évolutions de la fatigue due aux efforts.

**Measurement and Linear Prediction of Hull Pressure Spectra on CFAV QUEST -
Results of Q210 - Volume I**

by

D.C. Stredulinsky, N.G. Pegg, L.E. Gilroy

Executive Summary

Introduction

Ship structural design and analysis is moving away from empirical static design wave balance and towards more rational methods involving computer modelling of the sea load and structural response. This is taking place in both naval and commercial sectors where tools such as the American Bureau of Shipping (ABS) SAFEHULL code for tankers are gaining popularity. The Hydronautics Section at DREA has been developing methods for prediction of realistic sea loads and their application to finite element models of the hull structure to predict fatigue and ultimate strength performance. Through cooperative research with the MARIN (Maritime Research Institute of the Netherlands) Cooperative Research Ships organization, a linear three-dimensional seakeeping code, PRECAL, was developed to predict pressure spectra for the ship hull operating in a seaway.

While there are a small amount of model scale data available, there are few, if any full scale data available for verification of the pressure load and structural response predictions from PRECAL and the DND finite element code VAST. CFAV QUEST Trial Q210 was designed to measure the pressure fields, the hull girder strains and the conditions in which they occurred, to determine if the computer code predictions were giving reasonable results. Data was gathered from an array of 38 pressure transducers outfitted below the waterline, several strain gauges, a wave buoy, a microwave over-the-bow wave height meter, a radar system for measuring wave scatter, and ship motions accelerometers. A series of both high (12 knots) and low (5 knots) speed 30 minute trial runs in a variety of sea conditions were undertaken in head, bow, beam, quartering and following seas.

Principal Results

This report presents comparisons of ship motions data and pressure spectra measured during the trials and those predicted by PRECAL. Comparison of ship motions is quite good, particularly after corrections were made for roll damping. Pressure spectra comparisons range from being very good to satisfactory. In general, PRECAL predictions of pressure spectra are acceptable for providing linear sea loads to finite element models for stress analysis. This is an encouraging step towards developing rational structural analysis and sea loads for naval vessels.

Significance of Results

The major development project, Improved Ship Structural Maintenance Management (ISSMM), and other CF hull system life cycle management initiatives, require the capability to predict realistic sea loads for CF vessels. The method employed in the program PRECAL is one possible option for providing load requirements for both fatigue and ultimate strength ship hull failure limit states. The PRECAL code is being integrated with the DND finite element code VAST to predict stress spectra at critical details in a ship hull structure. These stress spectra can be used to predict fatigue crack initiation and crack growth behaviour for a given operating profile of a vessel. The PRECAL results can also be used with extremal theory to establish the most likely maximum loads on the hull structure to determine safety levels against ultimate strength.

Future Plans

The second phase of analyzing the Q210 results will address the measured versus predicted stress spectra at specific locations in the hull, and will be described in a later report. Integration of PRECAL and other sea load codes with structural analysis to predict endurance and strength capabilities of CF vessels will continue, mainly under the ISSMM project. Nonlinear sea loads such as slamming and whipping are not considered in the PRECAL analysis. Nonlinear time domain codes are being developed which will be able to consider the effects of nonlinear sea loads.

This report is presented in two volumes with Volume I containing the main body and Volume II containing the Appendices. Volume I will be given full distribution with Volume II being distributed only on request.

Contents

Abstract	ii
Résumé	ii
Executive Summary	iii
1 Introduction	1
2 Description of Q210 Trial	2
2.1 Instrumentation and fit out	2
2.2 Data acquisition	6
2.3 Trials plan	6
2.4 Trials log	6
3 The Three Dimensional Linear Seakeeping Program - PRECAL	9
4 Directional Wave Spectra	9
4.1 Selection of spectra and trial runs for analysis	9
4.2 Directional spectra for trial runs	13
5 Ship Motion Data	16
5.1 Pitch motion in head sea runs	17
5.2 Roll motion in beam sea runs	20
6 Hull Pressure Analysis	23
6.1 PRECAL pressure transfer function predictions	25
6.1.1 Irregular frequency suppression	25
6.1.2 Effect of roll damping on hull pressure predictions	28
6.2 Hull pressure prediction	28
6.2.1 RMS pressures	33
6.2.2 Pressure spectra	40
7 Summary and Conclusions	49
Acknowledgments	50
References	51
Appendices	Vol II
A Directional Wave Spectra	Vol II
B PRECAL Analysis	Vol II
C Comparison of Measured and Predicted Pressure Spectra	Vol II

1 Introduction

Traditional ship structural analysis is based on a static equivalent beam analysis of the ship hull girder balanced on a design wave. The safety factor separating the applied load and the structural resistance has been derived over time through trial and error influenced by the sometimes opposing forces of concern for safety and economic efficiency. The result is an analysis process which works for conventional ship structures, but greatly oversimplifies a complex loading-response process and does not provide the rational means to assess safety or develop more efficient designs.

Recent advances in computing technology have resulted in improved methods for modelling the loads acting on a ship operating in a defined seaway and the corresponding response of the complex ship structure. Both naval and commercial sectors are developing tools (such as the American Bureau of Shipping (ABS) SAFEHULL code for tankers) to bring rational ship structural analysis to reality. The Hydronautics Section at DREA has been developing methods for prediction of realistic sea loads and their application to finite element models of the hull structure to predict fatigue and ultimate strength performance. Through cooperative research with the MARIN (Maritime Research Institute of the Netherlands) Cooperative Research Ships organization, a linear three-dimensional seakeeping code, PRECAL, was developed to predict pressure spectra for the ship hull operating in a seaway. The PRECAL code has been used in conjunction with the DND finite element code VAST to predict stress spectra at critical details in the ship hull. These stress spectra can be used to predict fatigue crack initiation and crack growth behaviour for a given operating profile of a vessel. The PRECAL results can also be used with extremal theory to establish the most likely maximum loads on the hull structure to determine safety levels against ultimate strength.

While there is a small amount of model scale data available, there are few, if any, full scale data available for verification of the pressure load and structural response predictions from PRECAL and VAST. CFAV QUEST Trial Q210 was designed to measure the pressure fields, the hull girder strains and the conditions in which they occurred, to determine if the computer code predictions were giving reasonable results. Data was gathered from an array of 38 pressure transducers outfitted below the waterline, several strain gauges, a wave buoy, a microwave over-the-bow wave height meter, a radar wave imaging system and ship motions accelerometers. A series of both high (12 knots) and low (5 knots) speed 30 minute trial runs in a variety of sea conditions were undertaken in head, bow, beam, quartering and following seas.

This report presents comparisons of ship motions data and pressure spectra measured during the trials and those predicted by PRECAL. Nonlinear sea loads such as slamming and whipping are not considered in the PRECAL analysis. Nonlinear time domain codes are being developed which will be able to consider the effects of nonlinear sea loads. The second phase of analyzing the Q210 results will address the measured versus predicted stress spectra at specific locations in the hull. This will be described in a later report.

This report is presented in two volumes with Volume I containing the main body and Volume II containing the Appendices. Volume I will be given full distribution with Volume II being distributed only on request.

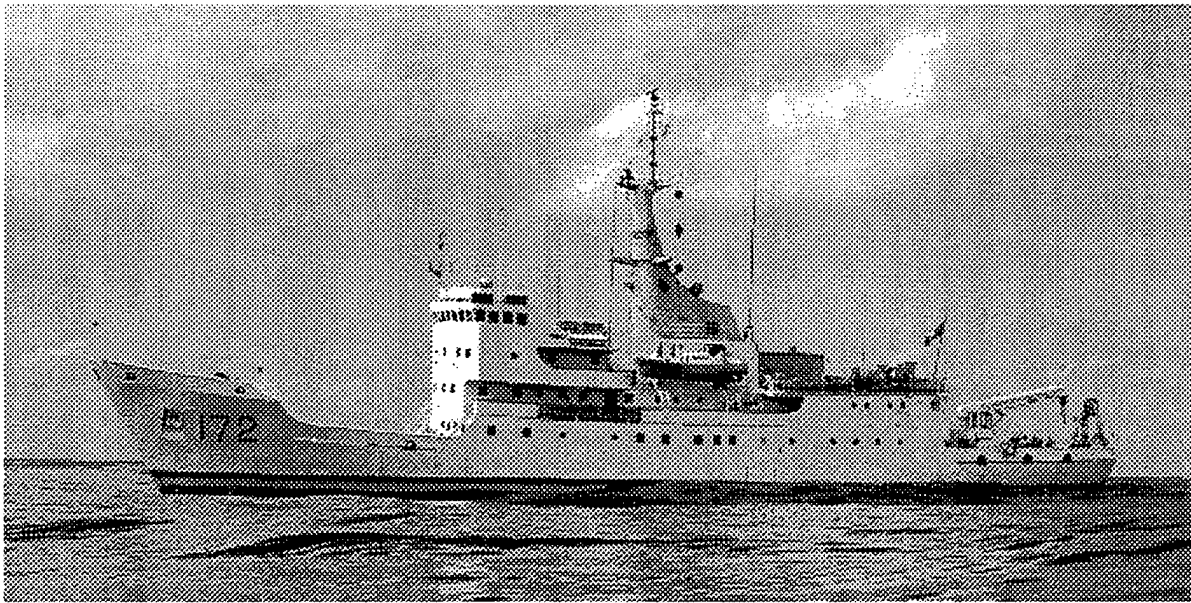


Figure 1: CFAV Quest

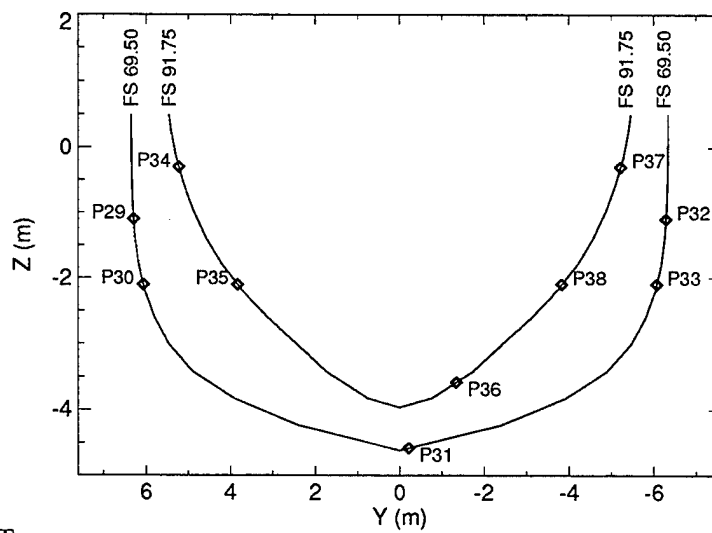
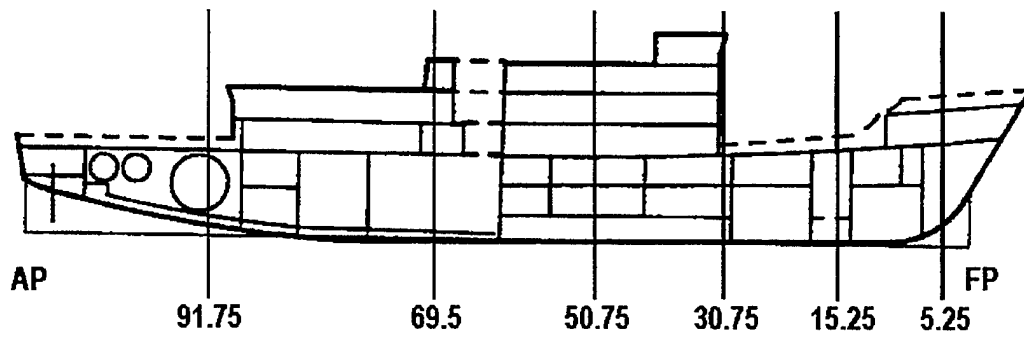
2 Description of Q210 Trial

CFAV QUEST trial Q210 was carried out by the Structural Mechanics Group of DREA during the period of November 4 to 18th, 1993 in the Atlantic Canada Maritime region. QUEST (see Figure 1) was instrumented to determine pressure distributions over the hull and corresponding strains in a variety of operating conditions. The purpose of the trial was to validate numerical predictions of pressure loads and structural response. In addition to the pressure loads and strains, it was also necessary to measure the sea state and ship operation as accurately as possible.

2.1 Instrumentation and fit out

The trial involved the installation of 38 pressure transducers of 4.75 mm diameter through the hull plating below the waterline. Transducer installation was done after the ship was removed from the water, by drilling and tapping a hole from the inboard side of the hull plating through which the transducer was placed. Locations are shown in Figure 2 at frame stations 5.25, 15.25, 30.75, 50.75, 69.5 and 91.75. The zero Z-coordinate is at the waterline. The transducers were installed as part of the QUEST docking in October 1993 in St John's Nfld. A total of 16 pressure transducers failed either before or during the cruise. Some were replaced and the trial was conducted with 32 working transducers.

In addition to the 38 small pressure transducers, 9 large (305 mm diameter) pressure transducers were mounted in the bow flare of QUEST above the waterline as shown in Figure 3. These larger transducers had been used on previous trials, Q150 and Q170, and were installed in existing recesses to measure slamming pressures, should slamming occur during the trials.



PORT

STBD

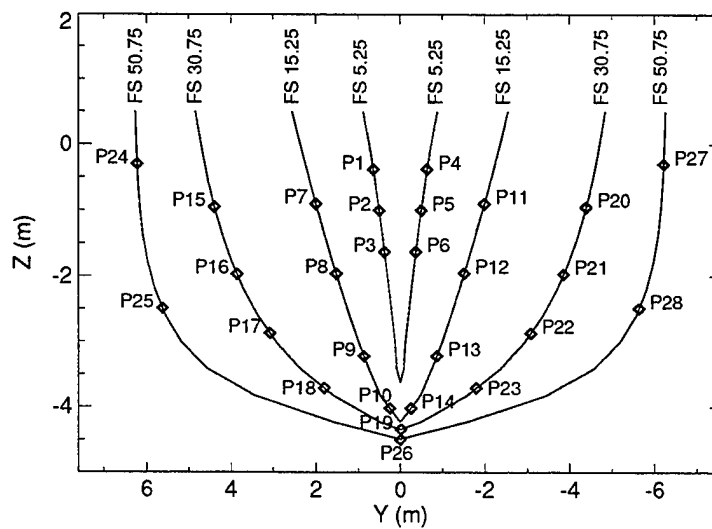


Figure 2: Locations of small pressure transducers on CFAV QUEST

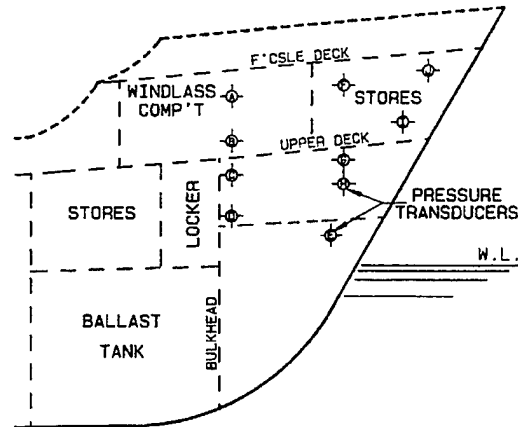


Figure 3: Locations of large pressure transducers on CFV QUEST

Eighteen strain gauges for measuring hull girder response were installed. Four gauges were placed in pairs on the two main deck girders and two on the keel in each of three locations along the ship (Figure 4).

The DREA ship motions measurements package was installed close to the ship CG and the ship's Non-Acoustic Data Acquisition System (NADAS) was used to give information on ship heading, position, and speed.

Wave height and direction measurement was done with the DREA Endeco Wavetrack directional wave buoy in a free float deployment each day. A TSK over-the-bow microwave wave height meter was also used to measure significant wave height and encounter period. A special boom had to be constructed to hold the unit over the bow. The TSK unit gave instantaneous readings of wave height in the lab. MacLaren Plansearch was contracted to use their 'MacRadar' system (calibrated based on TSK measurements) to determine wave direction using the ship's radar. The MacRadar unit proved useful in determining predominant wave direction during confused seas. The MacRadar system used the NADAS ship ground speed and direction data to correct for ship velocity. The NATWAV spectral ocean wave model, run in hindcast mode by MacLaren Plansearch, using wind field data provided by METOC, was also used to predict sea spectra.

The Wavetrack buoy and the MacRadar measurement systems are very different approaches to measuring wave spectra and hence there are differences in the results. The Wavetrack buoy samples at a specific point for 20 minutes to produce a spectra whereas the MacRadar samples data over a 1.5 nautical mile radius over a shorter period, of the order of a minute, to produce a spectra. The frequency results of the MacRadar system are also somewhat uncertain as the NADAS information was not always sampled at the same time that the MacRadar data was taken.

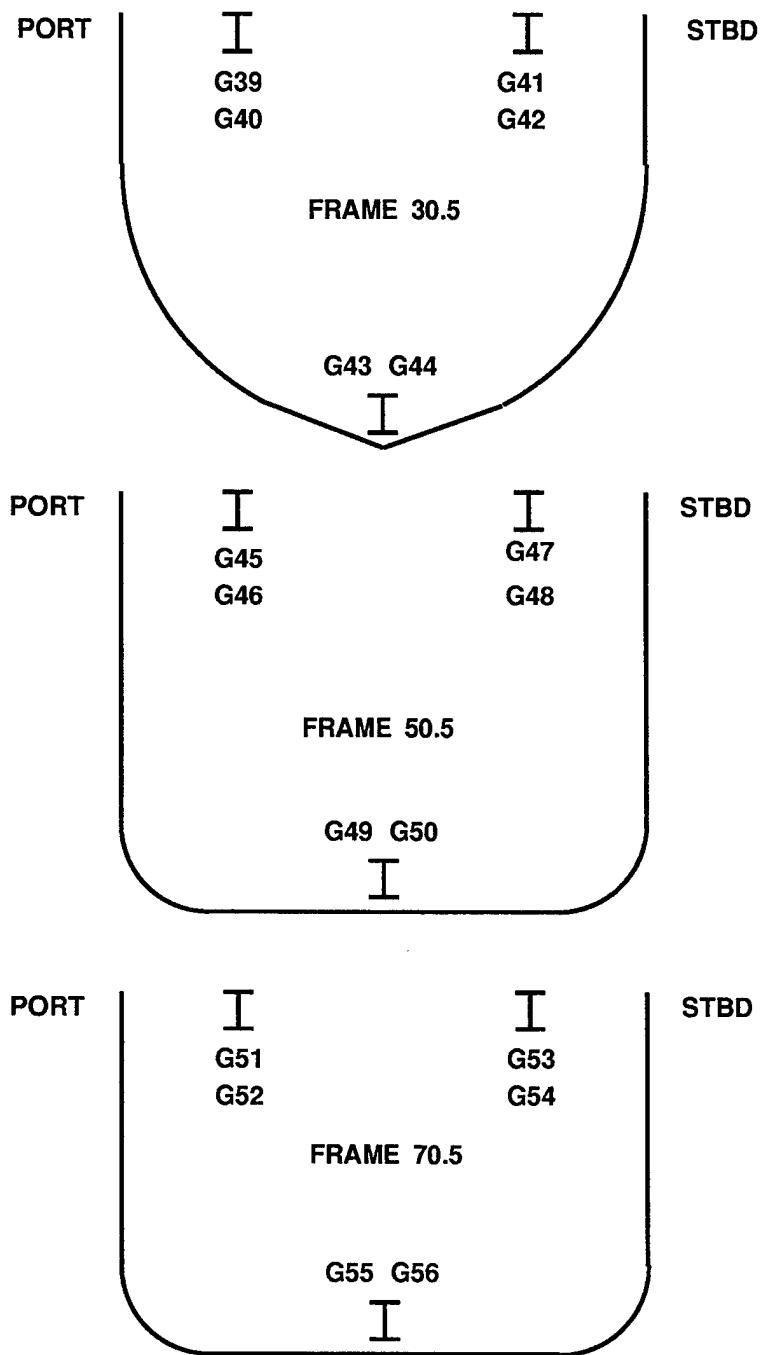


Figure 4: Locations of strain gauges on CFAV QUEST

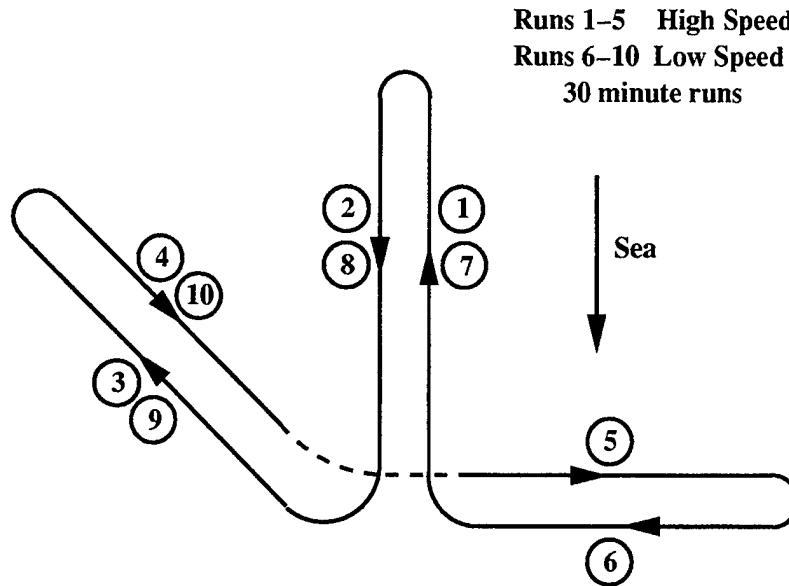


Figure 5: Operating pattern for Q210 trials

2.2 Data acquisition

The primary data acquisition system was three XR9000 TEAC 28 Channel VHS recorders. PC Labview software was used to monitor the data as it was being collected and for analyzing the data after collection. The tape recorders worked well without any failures. The Labview-based program was a great asset to Q210 over what was available for the previous Q170 and Q150 trials. It enabled real time monitoring and analysis of the data, something which we had previously been unable to do. The PC was able to handle the large number of channels and acquisition rate and undertake statistical and frequency analysis during each 30 minute run.

2.3 Trials plan

A daily operating pattern as shown in Figure 5 was used to meet the speed and heading matrix for each sea state. The wavebuoy was deployed in a free-float format at the beginning of each day and recovered at the end of the day. The operating pattern was undertaken in the vicinity of the buoy. On days when the sea state was low the full seakeeping pattern was not run and in some cases of high sea states the wavebuoy was deployed only for short periods of time to enable recovery.

2.4 Trials log

Tables 1 and 2 give the recorded log of the trials undertaken during Q210 including run number, ship heading, ship speed, wind direction and speed, visual observations of wave height and direction, and the significant wave measure by the Wavetrack buoy. The ship draft was 4.9 m (forward) and 5.2 m (aft) during the trial.

Table 1: Q210 Trial Run Summary - Part 1

Run No.	Date	Local Time		Ship Heading (True N.)	Ship Speed (knots)	Wave Direction (Visual)	Visual Wave Ht. (m)	Wave buoy Sig. Wave Ht. (m)
		Start	End					
1	Nov. 10	8.20	8.50	260	11	Head	1	1.0
2		8.56	9.27	80	11	Follow	1	1.0
3		9.31	10.00	215	11	Bow Stbd	1	0.9
4		10.07	10.37	35	11	Qtr Port	1	0.9
5		10.40	11.11	350	11	Beam Port	1	0.9
6		11.26	11.56	170	5	Beam Stbd	1	1.0
7		12.47	13.19	260	5	Head	1	1.0
8		13.28	13.58	80	5	Follow	<1	1.0
9		14.04	14.20	215	4	Bow Stbd	<1	1.0
10		14.26	14.42	35	4	Qtr Port	<1	1.1
11	Nov. 11	8.36	9.07	100	10	Head	2+	1.9
12		9.16	9.47	280	12	Follow	2+	1.9
13		9.51	10.22	45	10	Bow Stbd	2+	2.2
14		10.29	11.00	225	11	Qtr Port	2+	2.2
15		11.05	11.35	180	10	Beam Port	3	2.1
16		11.44	12.14	330	5	Beam Stbd	2+	2.2
17		12.24	12.54	60	5	Head	3-3.5	2.2
18		13.04	13.34	240	5	Follow	3	2.1
19		13.45	14.15	40	6	Bow Stbd	3	2.2
20		14.49	15.20	220	6	Qtr Port	2+	2.1
21	Nov. 12	8.37	9.08	300	12	Head	1.5-2	1.8
22		9.15	9.45	120	11	Follow	1.5	1.8
23		9.53	10.23	255	11	Bow Stbd	1-1.5	1.6
24		10.30	11.00	75	11	Qtr Port	1-1.5	1.6
25		11.07	11.37	30	11	Beam Port	1-1.5	1.6
26	Nov. 13	8.23	8.53	310	10	Head	3-4	3.3
27		9.00	9.31	130	12	Follow	3-4	3.7
28		9.35	10.05	265	11	Bow Stbd	3-4	3.7
29		10.10	10.40	85	11	Qtr Port	4	4.1
30		10.49	11.20	40	11	Beam Port	4	4.2
31		12.19	12.49	220	5	Beam Stbd	4+	4.1
32		14.25	14.55	310	4	Head	4+	4.2

Table 2: Q210 Trial Run Summary - Part 2

Run No.	Date	Local Time		Ship Heading (True N.)	Ship Speed (knots)	Wave Direction (Visual)	Visual Wave Ht. (m)	Wave buoy Sig. Wave Ht. (m)
		Start	End					
33	Nov. 13	15.01	15.31	130	5	Follow	4+	3.9
34		16.00	16.30	280	10	Bow Stbd 30	4+	n/a
35		17.21	17.52	265	6	Bow Stbd	3-4	n/a
36		18.01	18.31	85	5	Qtr Port	3-4	n/a
37	Nov. 14	8.22	8.52	220	10	Head	1.5	1.6
38		8.58	9.28	40	11	Follow	1.5	1.6
39		9.38	10.08	175	11	Bow Stbd	1.5	1.6
40		10.14	10.45	355	11	Qtr Port	1.5	1.6
41		10.54	11.25	310	11	Beam Port	1.5	1.6
42		15.57	16.27	165	7	Head	1.5	n/a
43		16.33	17.04	345	8	Follow	n/a	n/a
44		17.19	17.49	300	8	Qtr Port	n/a	n/a
45		17.58	18.28	120	8	Bow Stbd	n/a	n/a
46	Nov. 15	8.06	8.36	240	10	Head	2	n/a
47		8.42	9.12	60	11	Follow	2	n/a
48		9.20	9.51	195	11	Bow Stbd	2	1.8
49		10.14	10.44	150	10	Beam Stbd	1.5-2	1.8
50		10.53	11.23	330	5	Beam Port	1.5-2	1.8
51		13.33	14.08	230	5	Head	1.5	n/a
52		14.10	14.40	50	5	Follow	1.5	n/a
53	Nov. 16	6.28	6.58	285	5	Head	3-4	3.4
54		7.05	7.35	105	5	Follow	3-4	n/a
55		8.01	8.31	285	11	Head	3-4	n/a
56		8.37	9.07	240	10	Bow Stbd	3-4	n/a
57		9.11	9.41	240	4	Bow Stbd	3-4	n/a
58		9.44	10.15	60	5	Qtr Port	3-4	n/a
59		10.20	10.50	60	12	Qtr Port	3-3.5	3.2
60		13.01	13.31	105	11	Follow	3-3.5	3.4
61		13.37	14.07	195	11	Beam Stbd	3-3.5	n/a
62		14.13	14.43	195	5	Beam Stbd	3-3.5	n/a
63		15.34	16.04	290	11	Bow Stbd 30	3-4	n/a

3 The Three Dimensional Linear Seakeeping Program - PRECAL

PRECAL is a suite of programs [1] which was developed by the Cooperative Research Ships organization run by the Maritime Research Institute of the Netherlands (MARIN). PRECAL calculates vessel motions and hull pressures in regular and random waves using three dimensional potential theory.

PRECAL calculates the square root of the pressure response amplitude operator ($\sqrt{\text{RAO}}$) for each of the elements (facets) into which the wetted surface of the hull has been discretized. Figure 6 shows the element discretization used for the PRECAL analysis of QUEST. The dark triangular areas, shown in the bow and stern views of the facet geometry, represent gaps between panels which occur where the longitudinal edges of adjacent transverse rows of facets are not aligned.

The pressure response amplitude operator (RAO) is defined as the square of the pressure response per unit wave height as a function of wave frequency associated with a particular ship speed and heading. The resultant pressure spectra on the hull panels are then calculated using the measured directional wave spectra and the $\sqrt{\text{RAO}}$ s from PRECAL.

4 Directional Wave Spectra

4.1 Selection of spectra and trial runs for analysis

The graphs in Figure 7 and Figure 8 show for each day the sampling periods for the directional wave spectra collected with the Endeco Wavetrack buoy. The sampling periods are represented by thick horizontal lines placed at the significant wave height which is shown on the vertical axis. The wave spectrum sample I.D number prefixed by the letter 'S' is shown above each line. The graphs also show the time periods for each trial run in the form of a box (dashed line). The label at the top of each box gives the run I.D. number prefixed with the letter 'R'. The wave buoy sampled for a period of seventeen minutes in each hour. The ship trial runs were typically 30 minutes in length with a few minutes between each run. Generally the wave spectrum closest to the run time period was selected for analysis of the run. The wave spectrum sample used in the analysis associated with a run is shown in the bottom of the box representing each run.

Only trial runs having wave spectrum samples within half an hour of the run periods were selected for initial analysis. The spectra are expected to be representative of sea conditions during the runs since significant wave heights between consecutive runs differed by only a maximum of 15 percent. There was one exception. With reference to Figure 7, the significant wave height for wave spectra S16 was double that obtained in subsequent hours. It was determined that the buoy was close to the ship during the S16 run, giving artificially high readings compared to the TSK and NATWAV values so that the spectra S17 is likely to be more representative of the sea conditions during run R21.

Initially spectrum S8, the last spectrum recorded on November 10, was used in conjunction with run R10, but as noted in the MacLaren Plansearch report [2] of the Q210 trial wave spectra, spectrum S8 is not realistic suggesting that possibly the buoy was taken out of the water before this sample was completed. Spectrum S7 was therefore assigned to run R10 instead

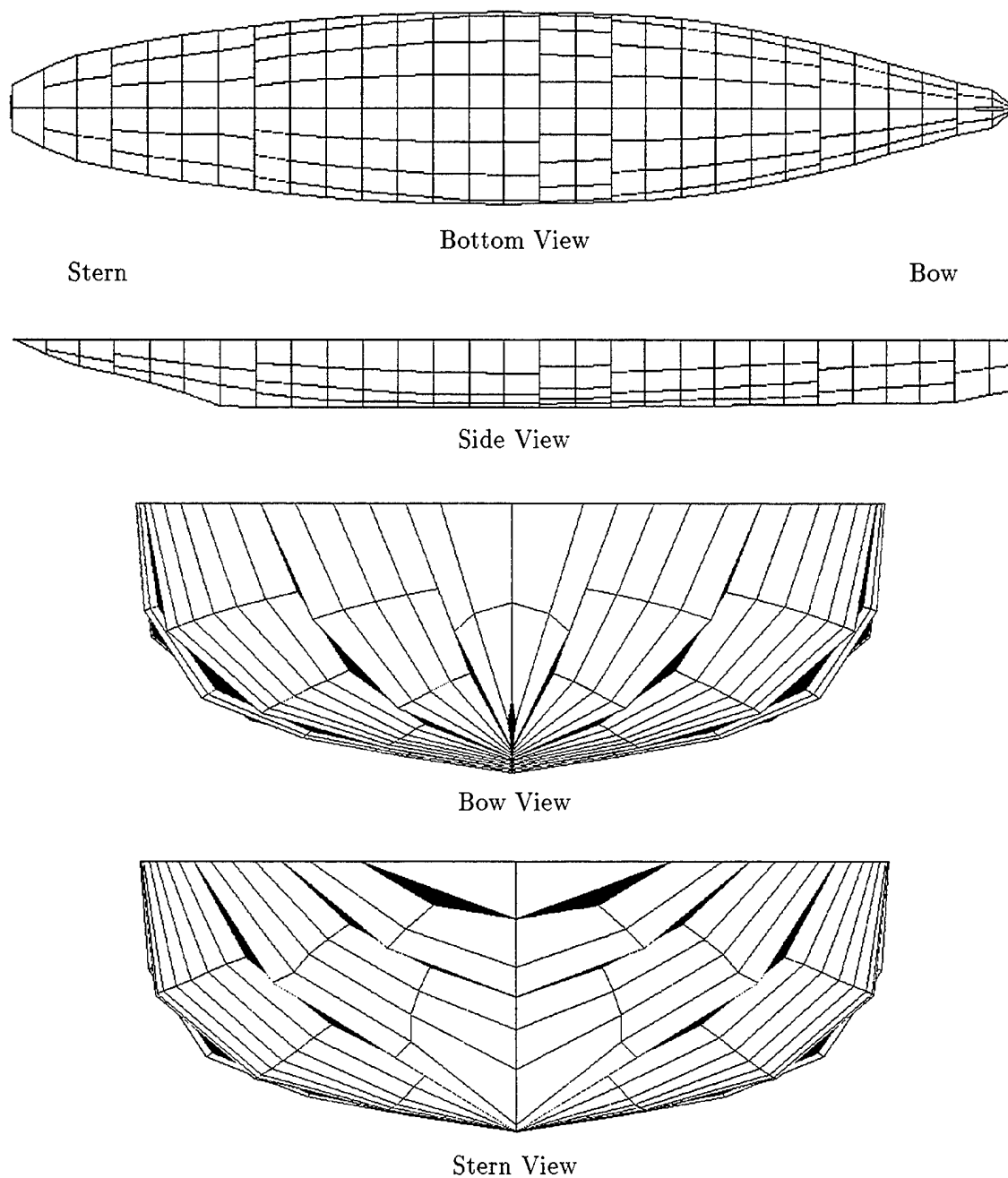


Figure 6: PRECAL hydrodynamic facet geometry (automatic generation)

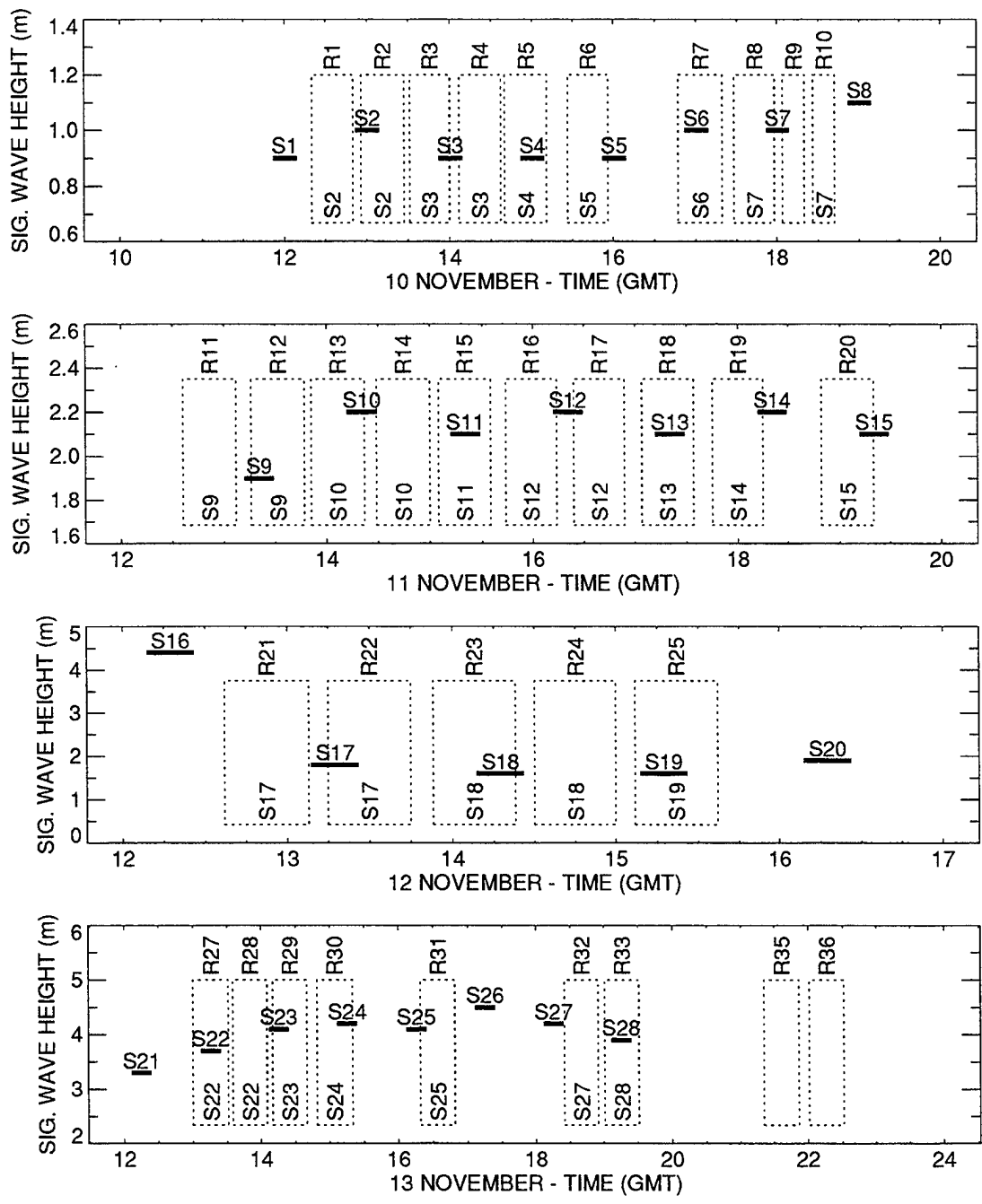


Figure 7: Comparison of time periods of Endeco Wavetrack buoy runs (S1-S28) and ship runs (R1-R36) for November 10,11,12 and 13, 1993

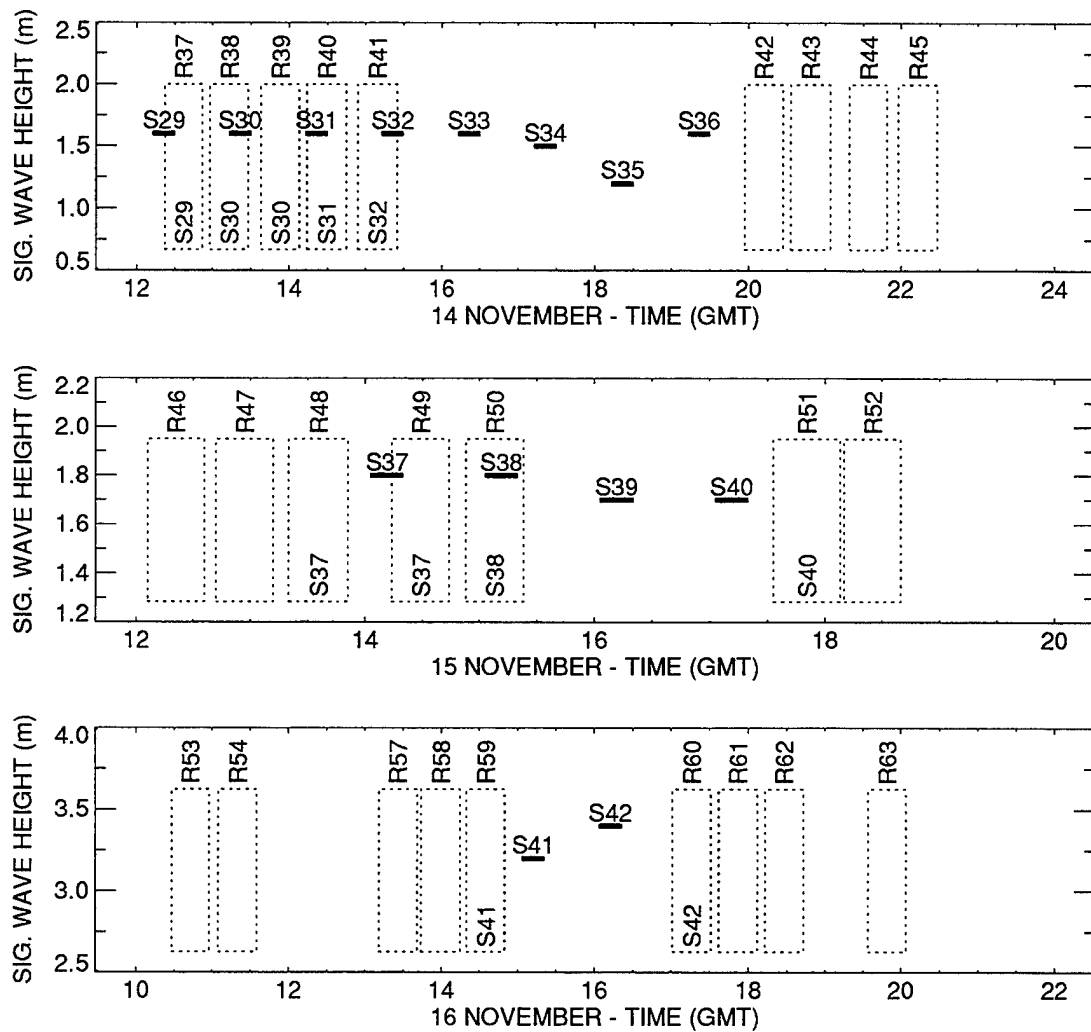


Figure 8: Comparison of time periods of Endeco Wavetrack buoy runs (S29-S42) and ship runs (R36-R60) for November 14,15 and 16, 1993

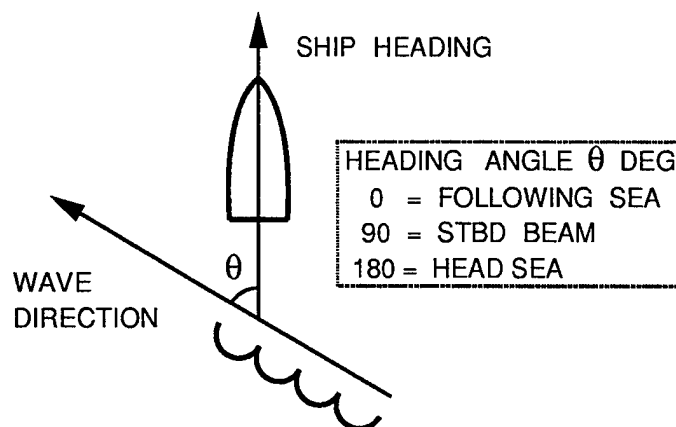


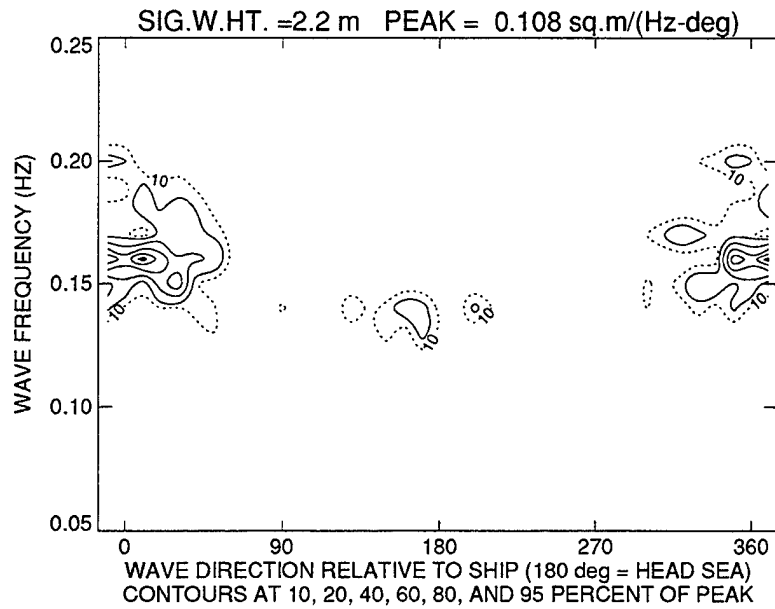
Figure 9: Definition of heading angle used in PRECAL

of spectrum S8.

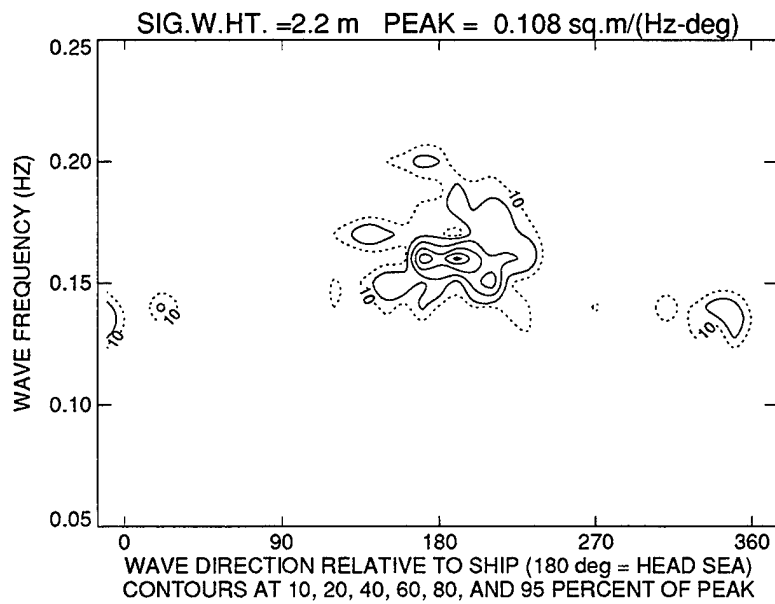
4.2 Directional spectra for trial runs

The directional wave spectra selected for analysis of trial runs (Section 4.1) are given in Appendix A. The wave power spectral density in $\text{m}^2/(\text{Hz-deg})$ is shown in contour plots as a function of wave frequency and wave heading angle relative to the ship orientation. The heading angle is defined in Figure 9. Initial examination of the spectra indicated that in some cases the observed wave headings during the trials did not match the plotted spectra but appeared to be shifted by 180 degrees as in the example shown in Figure 10. This trial run was for a head sea (see Run R17, Table 1) whereas the original spectrum shown in Figure 10a indicates a following sea condition. Shifting the spectrum heading by 180 degrees results in the plot shown in Figure 10b which is in agreement with the observed head sea condition during the trial.

Past experience has shown cases where the wave buoy headings have been in error by 180 degrees. The data from November 11 which encompassed run numbers 12 to 20 appears to suffer significantly from this problem. Figure 11 from reference [2] shows the comparison of the Wavetrack and MacRadar wave spectra for November 11. The results from the NATWAV hindcast model are also shown where available. It is evident that the Wavetrack data has two strong components separated by 180 degrees whereas the MacRadar data has only one strong component. In looking at the comparisons of the measured and predicted motion and pressure spectra in later Sections and in the Appendices of this report, the predictions show significant results at two frequency components; one corresponding to the predominant measured result, and a second corresponding to wave energy which is shifted in heading by 180 degrees compared with the predominant measured response. It is very likely that this additional peak, which is not found in the measured results, is a function of incorrect heading results from the Wavetrack wavebuoy. Analysis of the data indicates that the same wave energy may be counted twice, once each in the correct and incorrect heading. Since this extra and/or incorrect wave energy appears to be a random occurrence it is not easily removed from the data and has not been, but the reader should keep this in mind when reviewing the results.



a) Original directional wave spectrum



b) Directional wave spectrum shifted 180 degrees

Figure 10: Example of Endeco Wavetrack buoy spectra with 180 degree heading error (Run R17, head sea)

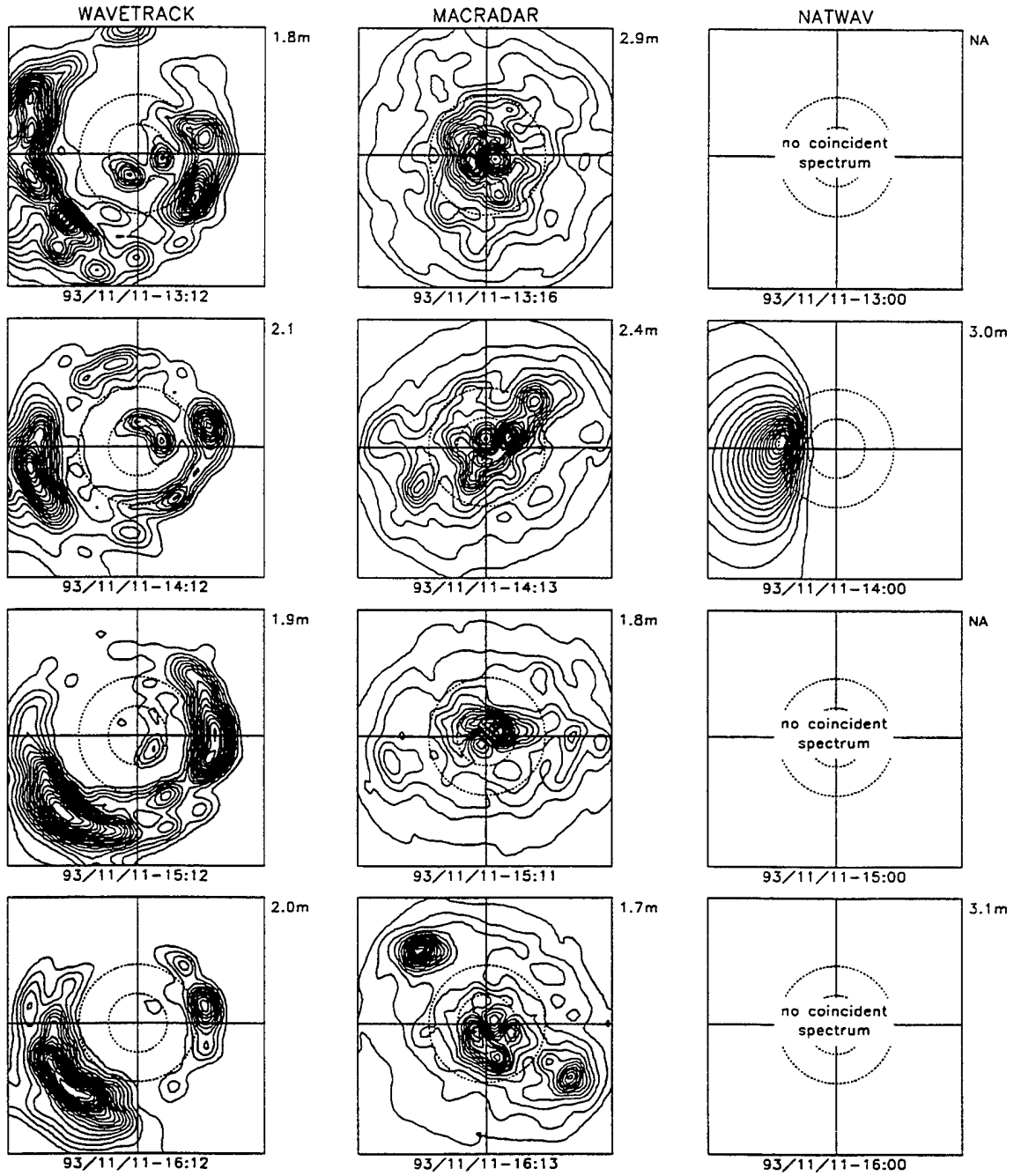


Figure 11: Comparison of Wavetrack, MacRadar and NATWAV Directional Wave Spectra for November 11, from Reference [2]. The spectra are presented with the direction from which the wave energy is coming plotted with North up and East to the right. Linear axes span -0.13 to 0.13 rad/m. Circles indicate 200 m (inner) and 100 m (outer) wavelengths. The significant wave height is shown at the upper right corner of each plot.

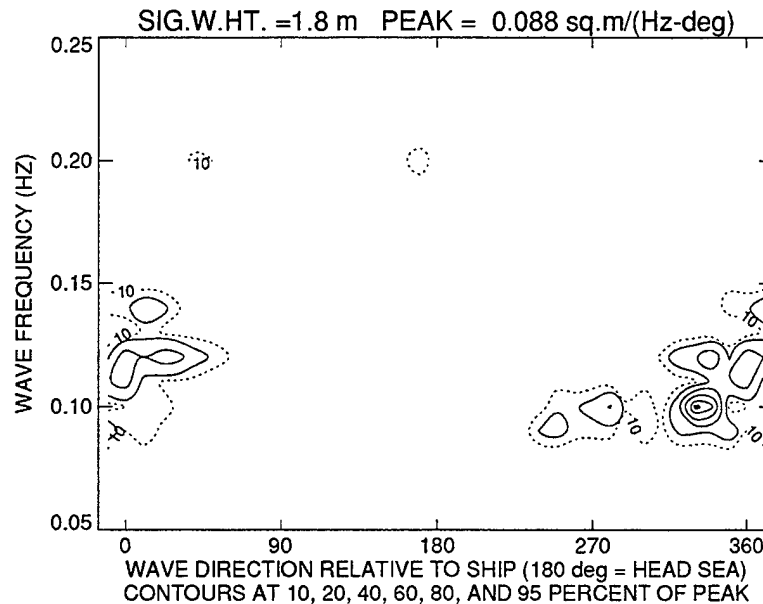


Figure 12: Endeco Wavetrack buoy directional spectra for Run R21

The situation for November 12 (runs R21 to R25 inclusive) is again different than November 11. For example, run R21 which was nominally a head sea run, was described visually as a 1.5-2 m head sea with a 6-7 second period combined with a 1m following wave of 6 second period. The directional spectra for this run (Figure 12), shows significant energy over a 180 degree sector, including following seas but no significant head sea component. After Run 21, the ship heading was reversed and the spectra for Run 22 which was nominally a following sea run, shows significant energy in the head sea region but no following sea component. Similar observations were made for the rest of the runs for November 12. Closer examination of the measured ship motion, strain and hull pressure spectra showed that the peak energy in the spectra for run R21 was at a lower frequency than for run R22, consistent with an encounter frequency shift assuming run R21 was a following sea run and run R22 was a head sea run. Similar trends exist for nominal bow and quartering sea runs, suggesting that for these runs the directional spectra may be correct and that the nominal headings do not represent the dominant wave direction. The remainder of the trial runs on other days were in reasonable agreement with the observed sea headings.

5 Ship Motion Data

Continuous ship motion time series data were available for each run. Time series data files with approximately 9000 points (30 minute period sampled at 5 Hz) were used for each run analysed. A single FFT analysis was conducted for each run using PV-WAVE [3], producing spectra with 0.0005 Hz resolution. Smoothed spectra were produced by combining groups of adjacent lines into 0.01 Hz bands, the same resolution provided in the wave buoy directional

spectra.

5.1 Pitch motion in head sea runs

To make a confirmatory check of predictions of ship motions, pitch alone was considered for six runs in nominal head seas. The pitch spectra were predicted by combining the Endeco Wavetrack buoy directional spectra and pitch response amplitude operator ($\sqrt{\text{RAO}}$) calculated with PRECAL. The wave spectra had a heading resolution of 10 degrees and a frequency resolution of 0.01 Hz. PRECAL was run for wave headings of 0 degrees to 350 degrees at 10 degree increments combined with wave frequencies of 0.03 Hz to 0.40 Hz inclusive at 0.01 Hz intervals for ship speeds of 5 knots and 11 knots. The pitch $\sqrt{\text{RAO}}$ was extracted from the PRECAL output files for each combination. The details of the PRECAL models and analysis are given in Appendix B. The pitch spectral density $S_p(f^e)$, where f^e is the encounter frequency, was obtained by calculating pitch 'energy' P_{ij} terms in rad^2 given by

$$P_{ij} = S_w(\theta_i, f_j^w) \left| H_p(\theta_i, f_j^w) \right|^2 \delta\theta \delta f^w, \quad (1)$$

where $S_w(\theta_i, f_j^w)$ is the directional wave spectral density ($\text{m}^2/\text{Hz-deg}$) and $\left| H_p(\theta_i, f_j^w) \right|$ is the amplitude of the pitch $\sqrt{\text{RAO}}$ (rad/m) at heading angle θ_i and wave frequency f_j^w . $\delta\theta$ is the heading angle spacing and δf^w is the wave frequency spacing. The encounter frequencies $f_{ij}^e(\theta_i, f_j^w)$ were also calculated. Bins of encounter frequency of δf^e width were set up and each pitch 'energy' term P_{ij} was added to the bin with centre frequency closest to the encounter frequency f_{ij}^e . The resulting pitch 'energy' spectra was divided by the encounter frequency bandwidth δf^e to obtain the pitch spectral density $S_p(f^e)$ with units of rad^2/Hz .

Initially the heading angle interval $\delta\theta$ and frequency interval δf were set to match the wave directional spectra spacings of 10 degrees and 0.01 Hz, respectively. Because of the coarse divisions, the distribution of energy to encounter frequency bins produced very jagged spectra. Smoother spectra were obtained by reducing the heading angle and frequency intervals and using linear interpolation of the original pitch $\sqrt{\text{RAO}}$ to obtain $\left| H_p(\theta_i, f_j^w) \right|$ and bilinear interpolation of the original directional wave spectra to obtain $S_w(\theta_i, f_j^w)$. It was found that subdividing the original heading angle and frequency intervals by a factor of four produced relatively smooth spectra and that further subdivision did not change the spectra significantly.

During the analysis it was discovered that integration of the wave buoy directional spectra over frequency and heading produced significant wave heights that were six to twenty percent lower than the Endeco Wavetrack buoy reported wave heights. The reason for this discrepancy is not known. The reported significant wave heights were in agreement with MacRadar and Natwav significant wave heights and are considered more reliable than the values obtained from the directional spectra. In all further analyses, the directional spectra components were multiplied by the appropriate factor so that the integration produced the correct significant wave height for each run. The predicted rms pitch values are compared to the measured rms values in Figure 13. Also shown are values predicted using the directional wave spectra in conjunction with the code SHIPMO6 [4]. The SHIPMO6 and PRECAL predictions are in very good agreement. The predicted and measured spectra are compared in Figure 14. The spectra are shown in terms of the square root of power spectral density with units of $\text{rad}/\sqrt{\text{Hz}}$.

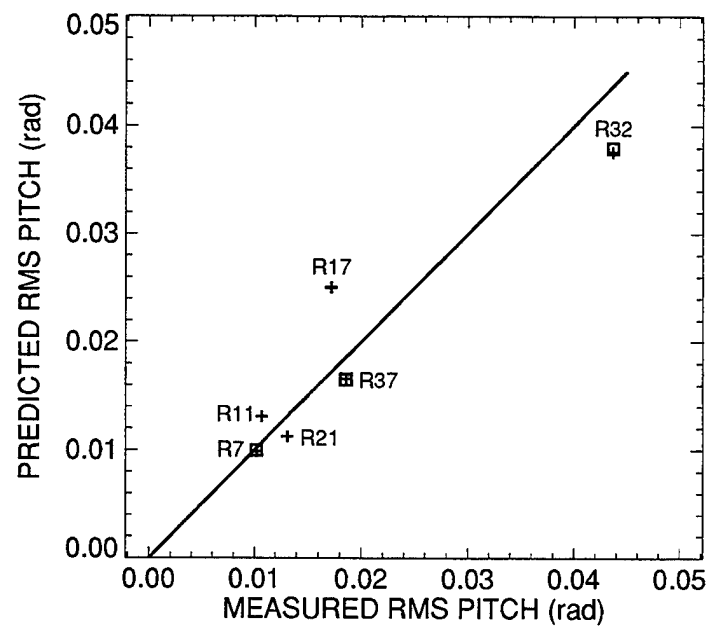


Figure 13: Comparison of predicted and measured rms pitch during head sea runs, + PRECAL, □ SHIPMO6

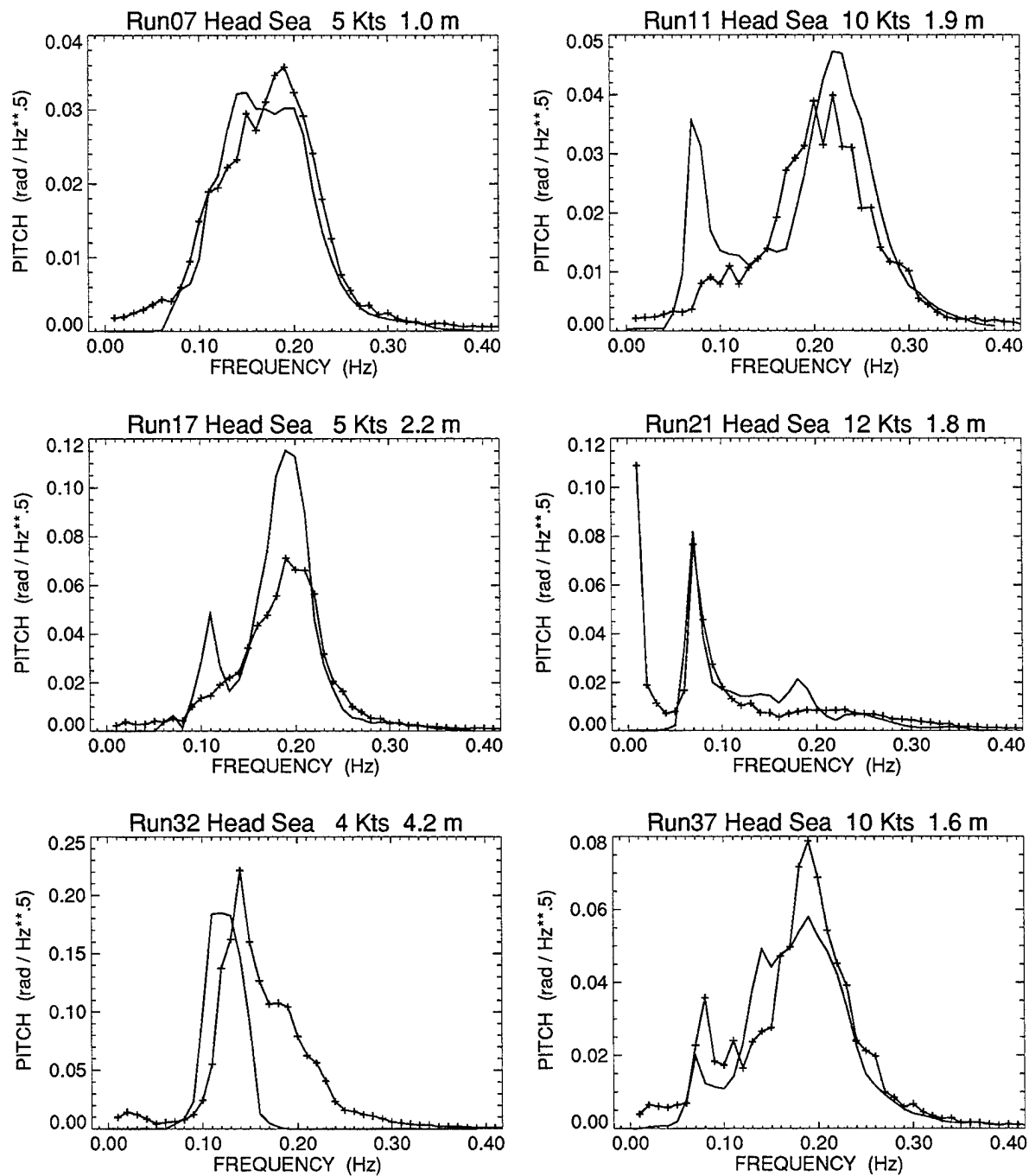


Figure 14: Comparison of measured and predicted pitch spectra, — Wavebuoy/PRECAL prediction, + Measured

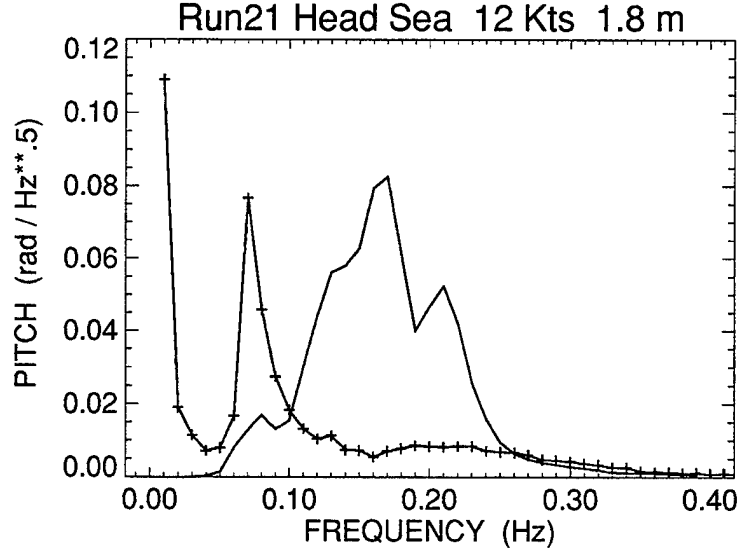


Figure 15: Comparison of measured and predicted pitch spectra for run R21 with wave spectra shifted 180 degrees, — Wavebuoy/PRECAL prediction, + Measured

Note that run R21, while nominally a head sea run, as indicated in section 4.2, contained the most wave energy in following seas, if it is assumed that the spectrum is correct and not shifted 180 degrees. The good agreement between the measured and predicted peak supports the assumption that the wave spectra for November 12 are correct and not shifted 180 degrees. If the spectrum is shifted 180 degrees to achieve a head sea condition, then the predicted pitch spectrum changes considerably as shown in Figure 15. The cause of the low frequency energy in the measured pitch for run R21 is not known.

5.2 Roll motion in beam sea runs

The present roll damping prediction in PRECAL is not considered to be very accurate. This was checked with the intention of modifying the roll damping as necessary to obtain correct roll motion before continuing on to the next stage; the prediction of hull pressures. The PRECAL input files contain a parameter DAMP which is normally set to 1.0. This multiplicative factor is applied to the diagonal roll damping term of the motion damping matrix. Coupled damping terms are not affected by the DAMP parameter. A plot of the predicted vs measured rms roll angles for a number of beam sea runs is shown in Figure 16 for normal PRECAL damping (DAMP=1.0) and for half of this damping value (DAMP=0.5). For comparison, lines with a slope of 1.0 (solid) and a slope of 0.5 (dashed) are shown. The graph shows that the initially predicted roll angles were half the measured values. Decreasing the damping by a factor of two gave much better agreement with measured roll.

The rms values excluded energy below 0.05 Hz for the reasons outlined as follows. The measured roll spectra contained significant energy below 0.05 (typically peaking between 0.01

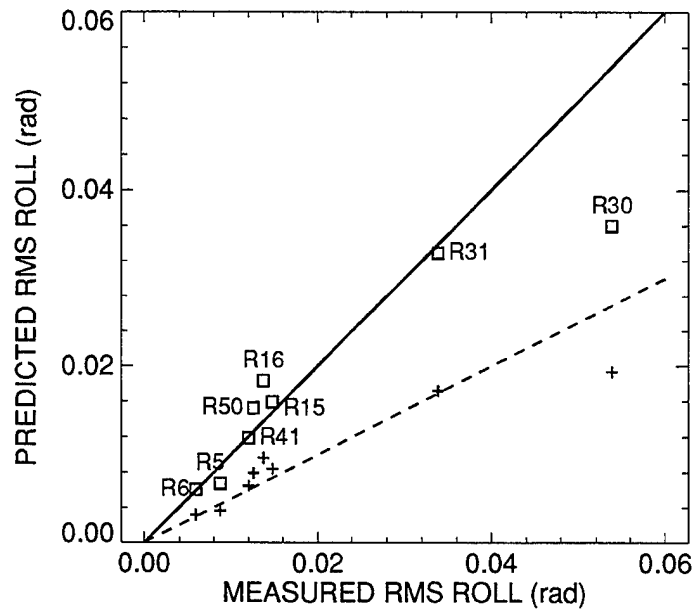


Figure 16: Comparison of PRECAL predicted roll and measured roll(rms) during beam sea runs, + Default roll damping, □ Roll damping reduced by a factor of two

and 0.015 Hz) which was not present in the measured directional wave spectra. Examination of other ship motion components showed that the low frequency peaks were also present in yaw and sway motions but not in surge, heave or pitch motions. It is suggested that these low frequency peaks were unlikely to be seaway related but likely due to repetitive rudder steering motions.

The predicted roll spectra for DAMP=0.5 are compared to measured roll spectra in Figure 17 and Figure 18. The PRECAL predictions were made in the same manner as used for pitch motion combining the roll $\sqrt{\text{RAOs}}$ and the directional wave spectra. Plots on the left side of graphs are for higher speed runs (10 or 11 knots) while those on the right are lower speed runs (5 knots). The high speed runs, and in some cases the low speed runs, show a peak at 0.08 Hz which is not predicted by PRECAL.

Figure 19 shows the regular wave roll $\sqrt{\text{RAOs}}$ predicted by PRECAL and SHIPMO6 in beam seas. The PRECAL $\sqrt{\text{RAOs}}$ were obtained for ship speeds of 5 and 11 knots. The SHIPMO6 $\sqrt{\text{RAOs}}$ were obtained for ship speeds of 0 and 11 knots. The PRECAL and SHIPMO6 predictions do not include the effect of the anti-roll tanks which were operating during the trial. The PRECAL $\sqrt{\text{RAO}}$ is shown for both the default damping (DAMP=1.0) and for half of the default damping (DAMP=0.5). An additional PRECAL prediction shown for a 5 knot ship speed is close to the 11 knot prediction. The PRECAL cases exhibit a much broader peak centered on a frequency approximately 50 percent higher than that predicted by SHIPMO6. The SHIPMO6 $\sqrt{\text{RAOs}}$ show peaks at 0.095 Hz, reasonably close to the measured peak of 0.08 Hz. A report on the tuning of the QUEST anti-roll tanks [5] reported the roll $\sqrt{\text{RAOs}}$ with

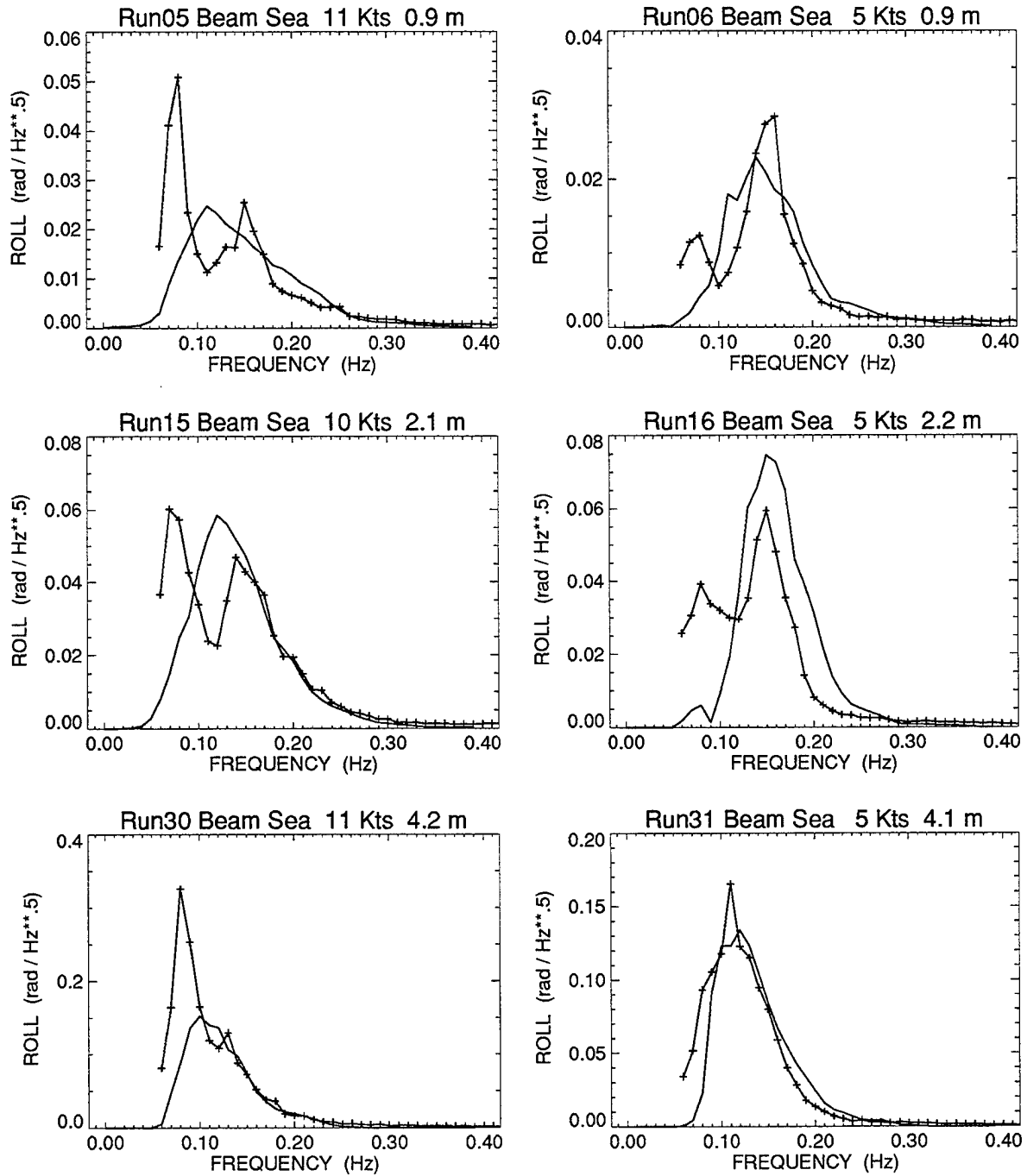


Figure 17: Comparison of measured and predicted roll spectra (Runs P5, P6, P15, P16, P30, P31), — Wavebuoy/PRECAL prediction, + Measured

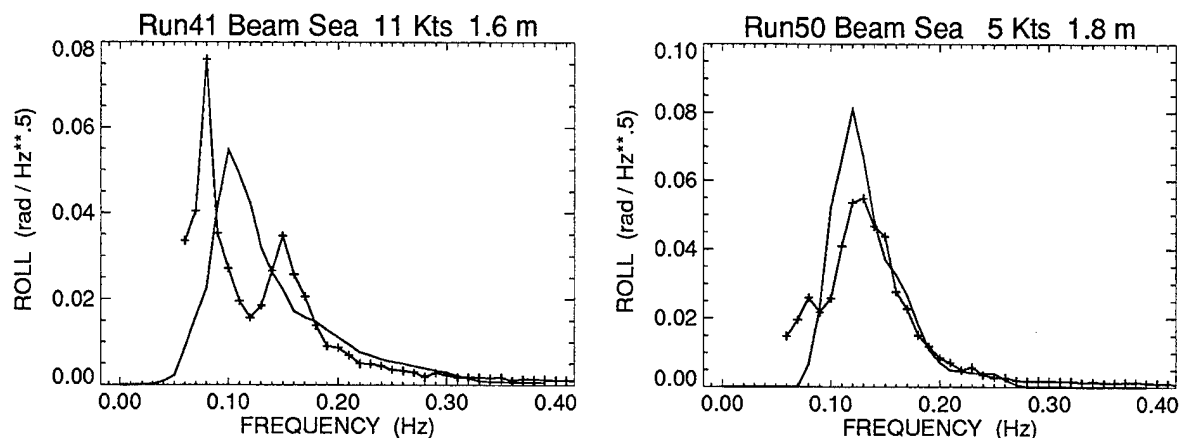


Figure 18: Comparison of measured and predicted roll spectra (Run R41 and run R50), — Wave-buoy/PRECAL prediction, + Measured

roll tanks empty and the ship stopped in $\lambda/30$ waves. Curves based on model test measurements and those derived from full scale data are shown. The full scale experiment shows a roll resonance near the same frequency and peaking at an amplitude of 20 percent higher than the SHIPMO6 zero-speed prediction.

Reference [5] does not give $\sqrt{\text{RAO}}$ s for the case of roll tanks in operation, claiming high statistical variability in the measured wave and roll spectra and the need for more data to determine the nonlinear effects which were thought to be significant for the roll tanks. An estimate of the roll $\sqrt{\text{RAO}}$ with anti-roll tanks in operation was made by comparing the measured wave and roll spectra from Reference [5] taken with the ship operating in beam seas (3.3m significant wave height) when stopped, moving at 5 knots and moving at 11 knots. The estimates based on the measurement are compared to the PRECAL $\sqrt{\text{RAO}}$ in Figure 20. The measured $\sqrt{\text{RAO}}$ s show a sharp peak near 0.07 Hz combined with broadband response at higher frequencies. The 0.07 Hz peak is significantly higher for the 11 knot case than for the 5 knot case. This is consistent with the differences between PRECAL predictions of roll and the measured roll spectra for the beam sea runs given in Figure 17.

Based on the above it was concluded that the peaks in the measured roll spectra near 0.08 Hz are realistic and attributed to a peak in the roll $\sqrt{\text{RAO}}$ at this frequency which is not contained in the PRECAL $\sqrt{\text{RAO}}$. The $\sqrt{\text{RAO}}$ s predicted by both SHIPMO6 and PRECAL do not include the effect of the anti-roll tank and it is not clear why these $\sqrt{\text{RAO}}$ s show peaks with a significantly lower amplitude than Reference [5] for tanks empty.

6 Hull Pressure Analysis

The hull pressures were predicted at 18 of the small pressure transducer locations for 39 of the trial runs. Pressure spectra were predicted at a given location for a given run by combining the wave buoy directional wave spectrum thought to best represent the run and the PRECAL

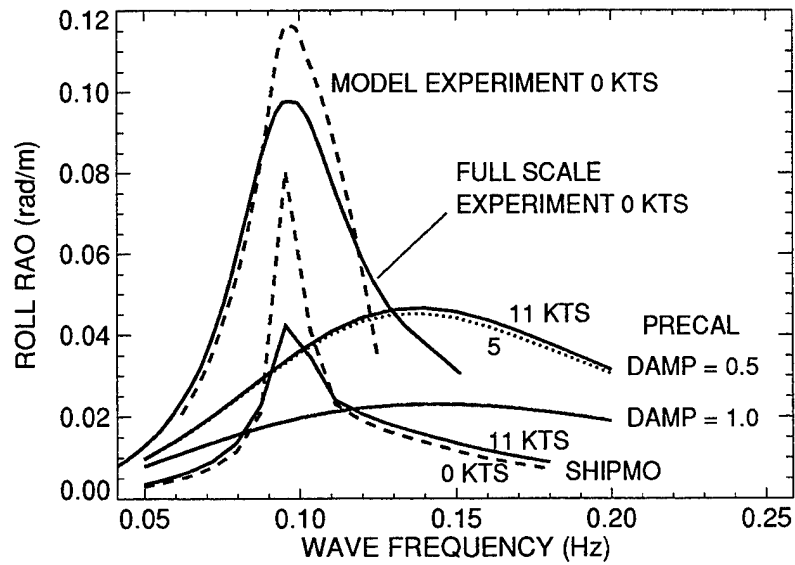


Figure 19: Comparison of beam sea roll $\sqrt{\text{RAOs}}$ with anti-roll tanks empty

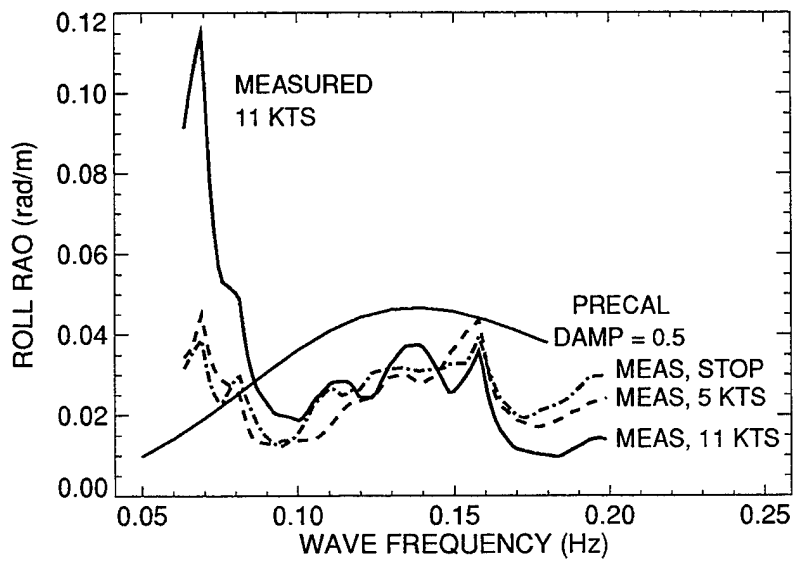


Figure 20: Comparison of the beam sea roll $\sqrt{\text{RAO}}$ predicted by PRECAL to measurements with anti-roll tanks in operation

hull pressure transfer functions for the location. This section first considers some aspects of the PRECAL pressure transfer function calculation and then discusses hull pressure prediction and comparison with trial measurements. Graphical results of all of the 18 prediction locations for the 39 runs are given in a separate Appendix to this report. Only a few representative comparisons are given in this main body of the report.

6.1 PRECAL pressure transfer function predictions

PRECAL was used to obtain the regular wave pressure transfer function amplitudes (pressure $\sqrt{\text{RAO}}$) given by the ratio of the pressure amplitude at a location on the hull to the wave amplitude in units of kPa/m. The pressure $\sqrt{\text{RAO}}$ s were predicted for wave headings from 0 degrees to 350 degrees inclusive at 10 degree increments for ship speeds of 5 knots and 11 knots.

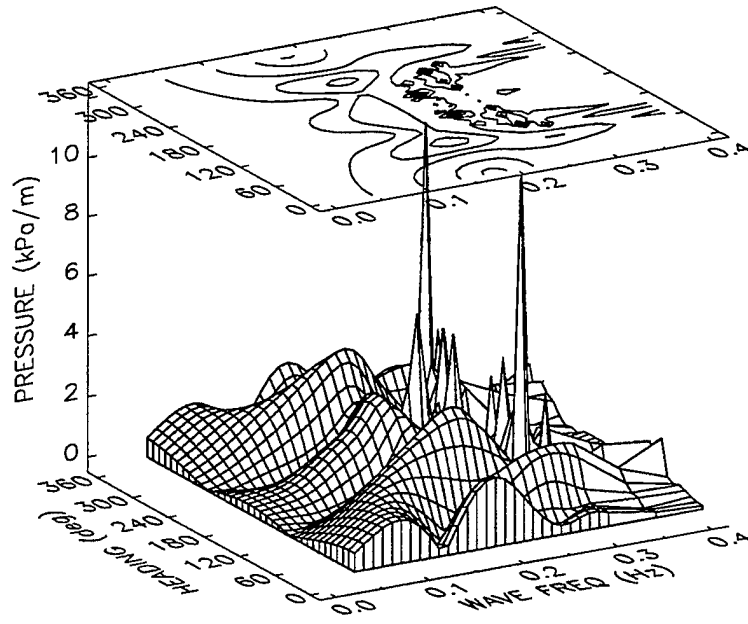
Wave frequencies between 0.03 Hz to 0.30 Hz inclusive at 0.01 Hz intervals and 0.35 Hz and 0.4 Hz were included in each $\sqrt{\text{RAO}}$. The pressure $\sqrt{\text{RAO}}$ s were predicted for 24 of the hull pressure transducer positions (locations P1, P2, P3, P4, P5, P6, P7, P8, P9, P10, P11, P12, P13, P14, P17, P18, P19, P22, P23, P26, P31, P35, P36, P38 of Figure 2). The pressure at each location was predicted with the PRECAL program using the WEIGHT option which calculates a weighted average of the pressures at the four closest hydrodynamic facets.

6.1.1 Irregular frequency suppression

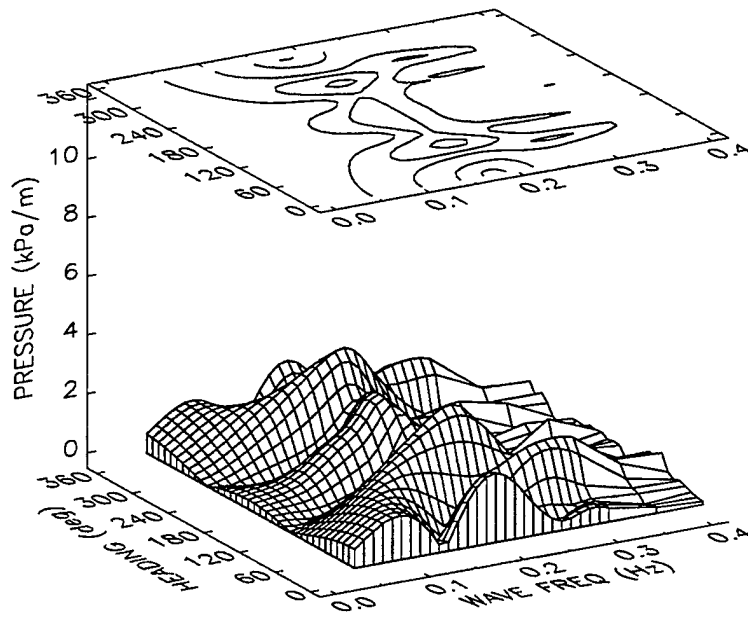
PRECAL contains an option to alleviate problems due to irregular frequencies. A free-surface panel distribution is added to the hydrodynamic hull mesh (activated by including the option record OFSP in the QUEST.CND input file) given in Appendix B. Two transverse panels per waterline facet were used for the suppression (FSPANS =2 in the QUEST.CND file). For comparison, runs with no suppression were also conducted.

At a speed of 5 knots, without suppression, very few spurious spikes occurred at the frame stations near the bow (FS 5.25 and FS 15.25). At locations further aft, many irregular frequency peaks were observed in the frequency range between 0.2 and 0.4 Hz and headings between 60 and 240 degrees as shown in Figure 21a for location P31. The suppression at the 5 knot speed was very good as indicated for location P31 in Figure 21b. At locations P17, P18, P19, P22, P23, P26 and P31, with irregular frequency suppression, a single spurious peak was observed at 0.35 Hz for a 180 degree heading. These peaks were similar to that shown for location P19 in Figure 22.

For the ship speed of 11 knots, at all transducer locations, extremely high peaks in the pressure $\sqrt{\text{RAO}}$ occurred at headings of 10 and 350 degrees for a wave frequency of 0.28 Hz. For this combination of speed, heading and wave frequency, the encounter frequency approaches zero, causing spurious peaks such as those shown in Figure 23 with and without irregular frequency suppression. Once the spurious peaks at the 0.28 Hz wave frequency were removed, the pressure $\sqrt{\text{RAO}}$ s could be viewed to check for irregular frequency peaks. The irregular frequency problem was found to be worse at 11 knots than at 5 knots. Spurious peaks occurred at all transducer locations both with and without suppression. Generally, the peaks became larger and more numerous at locations further aft. Figure 24 shows an example of the pressure $\sqrt{\text{RAO}}$ surface for transducer 26 with and without suppression. The suppression generally reduced the number and height of the spurious peaks; however, many peaks still remained and



a) Without suppression



With suppression

Figure 21: Effect of irregular frequency suppression on the pressure $\sqrt{\text{RAO}}$ at location P31 for a 5 knot ship speed

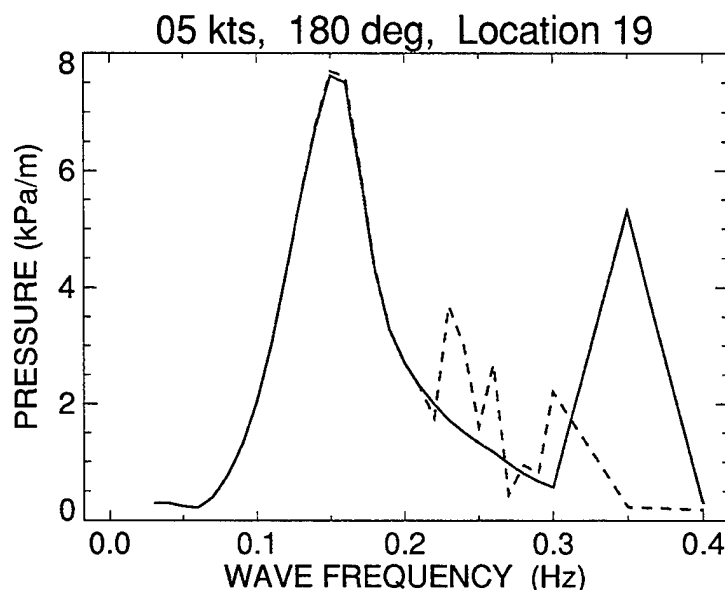


Figure 22: Effect of irregular frequency suppression on the pressure $\sqrt{\text{RAO}}$ at location P19 with head seas and a 5 knot ship speed; - - - without suppression,— with suppression)

tended to be concentrated at higher frequencies and closer to a 180 degree heading angle (head seas) than for the case with no suppression.

Generally, the irregular frequency suppression removed the spurious peaks without changing the rest of the pressure $\sqrt{\text{RAO}}$ curve. At locations near the bow in beam sea runs, the suppression also caused a shift of the higher frequency portion of the curve for both the 5 knot and 11 knot cases as shown in Figure 25 for 5 knots. For the case of following seas the irregular frequency suppression had no effect on the pressure $\sqrt{\text{RAO}}$ curves as shown in Figure 26 for Location P31 for 11 knots. The curve contains a spurious peak at 0.28 Hz which was not changed by the irregular frequency suppression and is likely a result of the close proximity of this point to the zero-encounter-frequency peaks at 10 and 350 degree headings. Similar results were obtained in following seas for 5 knots.

A PV-WAVE procedure called TRANSEDIT was written and used to view and edit the PRECAL pressure $\sqrt{\text{RAO}}$ s to remove spurious peaks. The procedure allows viewing of the 3D pressure $\sqrt{\text{RAO}}$ surface for each transducer location for a selected speed as a function of frequency and heading in a format similar to that used in Figure 24. At a selected frequency, a 2D graph of the pressure $\sqrt{\text{RAO}}$ vs heading can be viewed and points selected and moved using a cursor controlled by mouse or track ball input. Curves at adjacent frequency values are also displayed for reference to assist in positioning of new points to create a smooth surface. In a similar manner, a heading angle can be selected and the curve which is displayed as a function of wave frequency, can be edited.

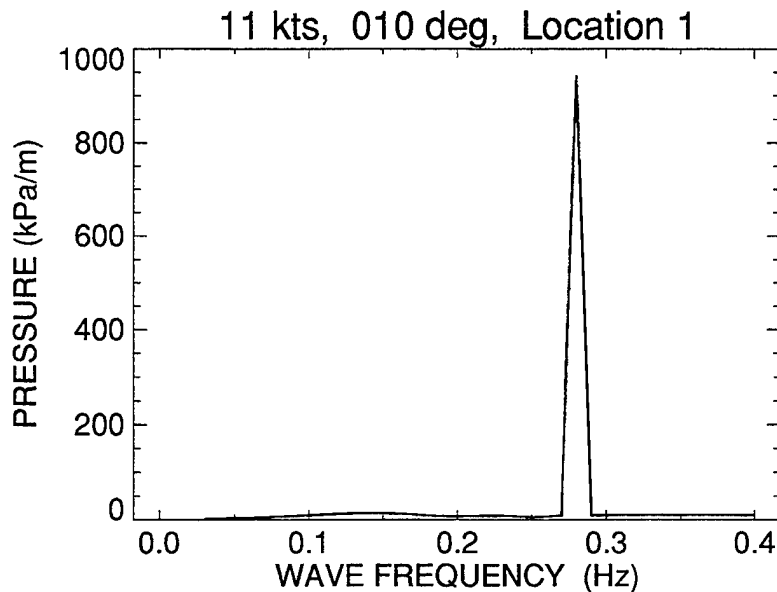


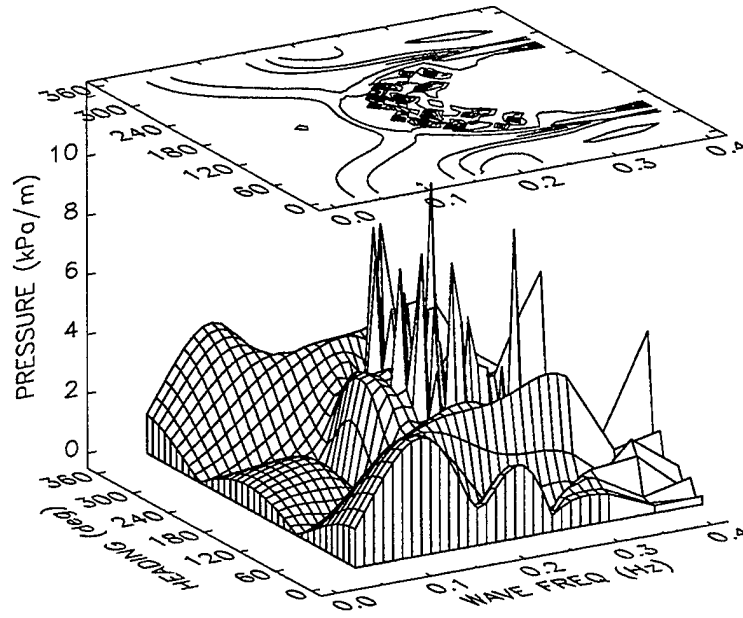
Figure 23: Spurious peak in the pressure $\sqrt{\text{RAO}}$ near a zero encounter frequency; - - - without irregular frequency suppression, — with suppression)

6.1.2 Effect of roll damping on hull pressure predictions

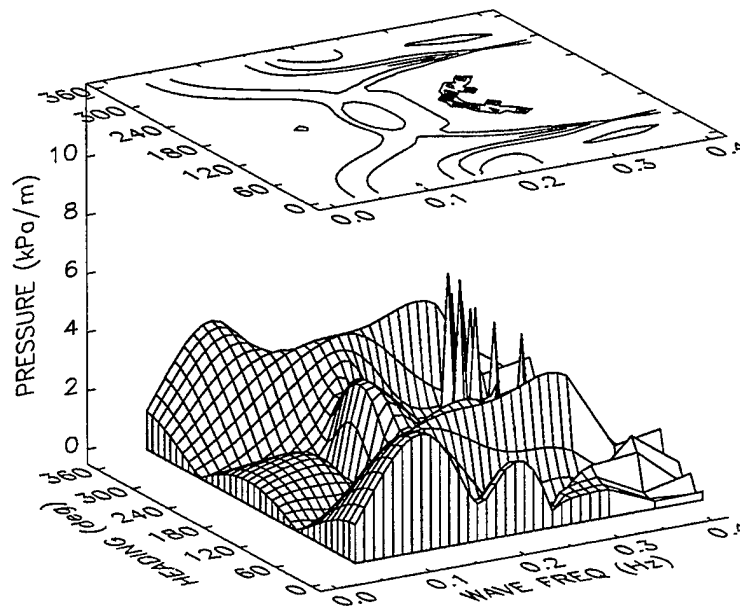
In section 5.2, it was shown that the PRECAL default roll damping needed to be halved in order to achieve reasonable agreement between predicted and experimental rms roll motions in irregular beam seas. The hull pressure $\sqrt{\text{RAOs}}$ were calculated for both the default PRECAL roll damping and the case where the roll damping coefficients were reduced by a factor of two (setting the parameter DAMP=0.5 in the QUEST.INP input file). Changing the roll damping had no effect on the hull pressure $\sqrt{\text{RAOs}}$ for head or following seas and only a small effect at other headings for keel locations and near the bow (FS 5.25 and FS 15.25). The differences were greatest, although still relatively small, at locations near the surface and further aft, and were similar for both the 5 knot and 11 knot ship speed cases. The maximum differences occurred close to beam seas (heading angles between 70 to 90 degrees and between 270 and 290 degrees depending on location). Figure 27 shows the maximum differences for transducer location P17 on the port side of the ship. Note that waves coming from the port side of the ship caused the pressures on the port side to increase when the roll damping was decreased (Figure 27b), but when the waves were switched to the starboard beam (Figure 27a), the pressures decreased when the roll damping was decreased. A similar trend was observed further aft as shown for location P35 in Figure 28.

6.2 Hull pressure prediction

The pressure spectra for a specific transducer location and a given run were predicted by combining the Endeco Wavetrack buoy directional spectra for the run, and the root pressure response amplitude operators ($\sqrt{\text{RAOs}}$) calculated with PRECAL. The PRECAL $\sqrt{\text{RAOs}}$ were



Without suppression



With suppression

Figure 24: Effect of irregular frequency suppression on the pressure $\sqrt{\text{RAO}}$ at location P26 for an 11 knot ship speed

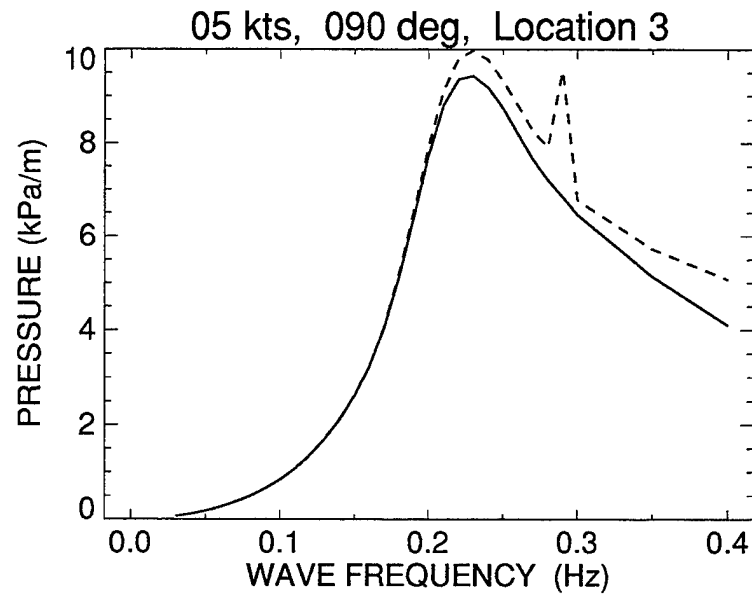


Figure 25: Shift in pressure $\sqrt{\text{RAO}}$ near bow with beam sea caused by irregular frequency suppression; - - - without suppression,— with suppression)

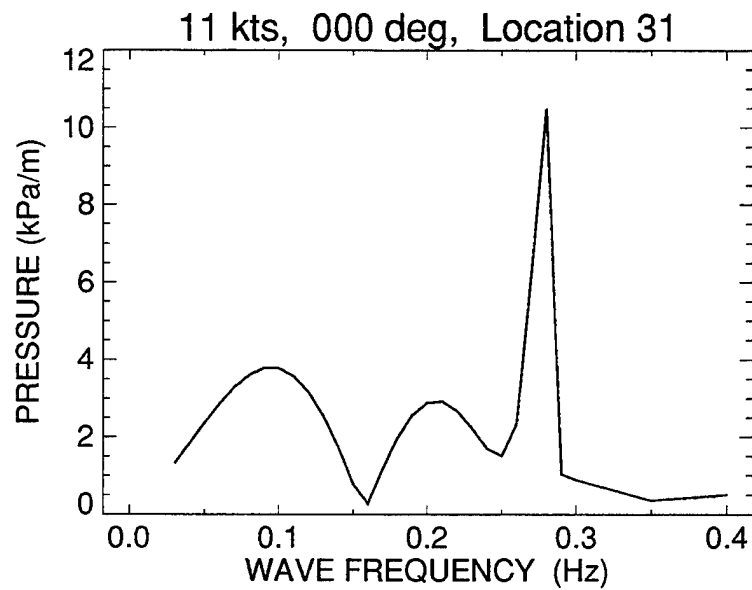
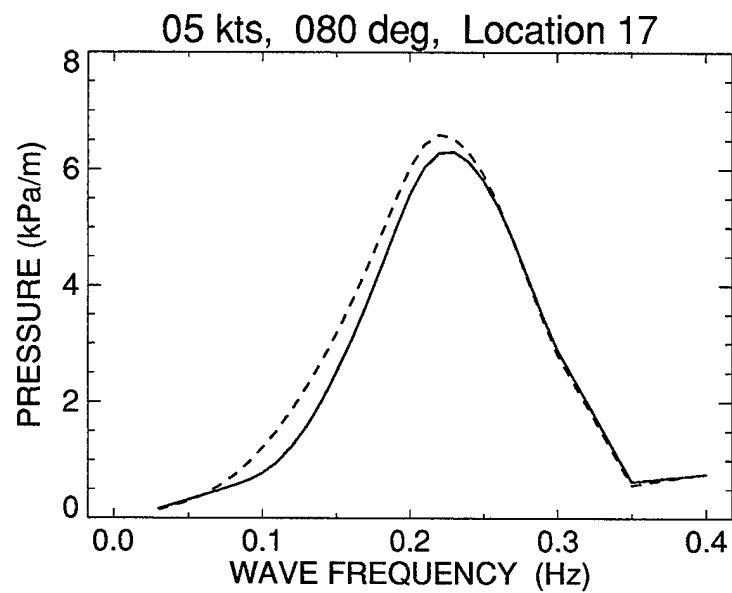
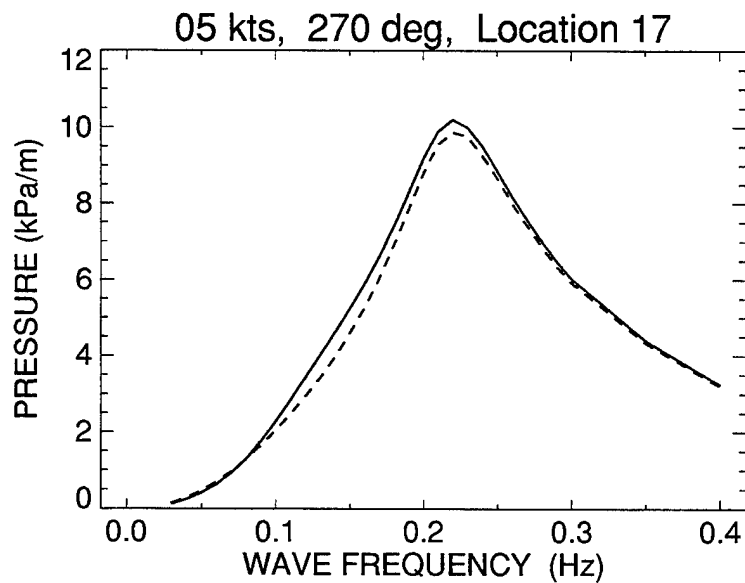


Figure 26: Example of pressure $\sqrt{\text{RAO}}$ in following sea; - - - without suppression,— with suppression)

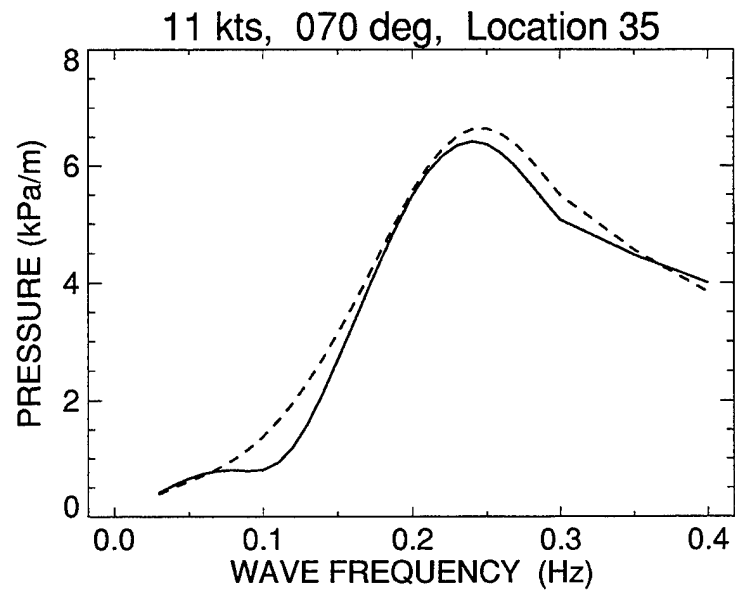


a) Location on side of hull sheltered from waves

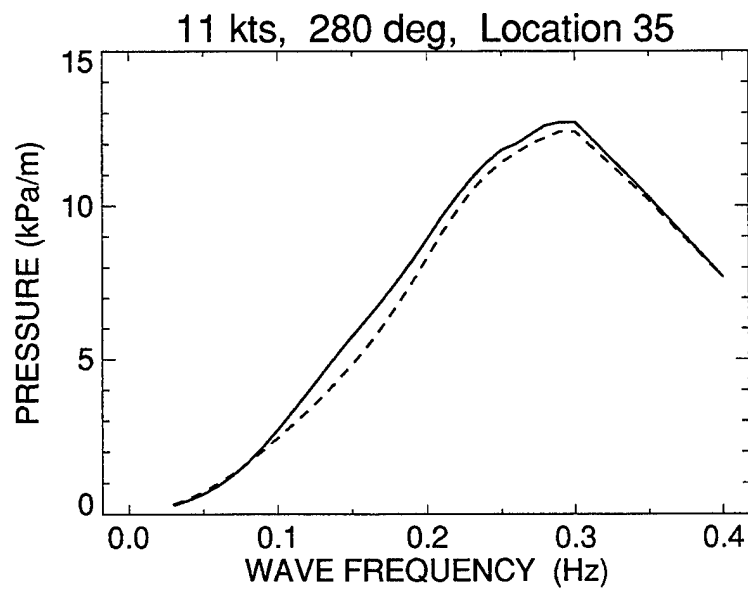


a) Location on side of hull facing into waves

Figure 27: Effect of roll damping on the pressure $\sqrt{\text{RAOs}}$ at location P17 for headings showing maximum differences; - - - default roll damping, — half damping)



a) Location on side of hull sheltered from waves



a) Location on side of hull facing into waves

Figure 28: Effect of roll damping on the pressure $\sqrt{\text{RAOs}}$ at location P35 for headings showing maximum differences; - - - default roll damping, — half damping)

calculated for the selected location in a manner identical to that used to predict the pitch and roll spectra considered in Section 5.1. To verify the PRECAL predictions of hull pressures, measurements from eighteen of the pressure transducer locations for each of 39 runs were considered.

6.2.1 RMS pressures

Plots of the predicted rms hull pressures, calculated from the predicted pressure spectra, versus the measured rms pressures are shown for each frame station in Figures 29 to 34. A dotted line indicating perfect correlation between measured and predicted pressure is also shown for reference on each plot. The plots are orientated with locations nearest the surface at the top of the figure and those closest to the keel at the bottom of the figure. Plots for locations at the same depth are shown side by side with the port location on the left side of the figure and the starboard location on the right. In Figure 29 the plots for locations P2 and P4 have not been included since the pressure transducers at these locations were not working properly during most of the trial. The plots for location P1 and P31 show fewer points than the other graphs because transducers at these locations were working for only part of the trial. The points are plotted with different symbols to distinguish between runs nominally for head, bow, beam, quartering or following irregular seas.

Examination of the rms pressure graphs show that there is better agreement between predictions and measurements for locations near the bow than for those further aft where the predicted pressures tend to be lower than the measured values. This was examined quantitatively by calculating least square linear fits to each graph. Initially a fit to a two-parameter model (the linear curve $y = ax + b$) was employed where y_i are the predicted pressure values and x_i are the corresponding measured values. This produced curves with slopes close to unity at frame station FS 5.25 but at station FS 15.25, slopes of about 0.75 were calculated with a significant y -axis intercept. A second fit to a one-parameter model was obtained with the equation $y = ax$ which forces a y -axis intercept of zero. This produced only marginally higher standard deviations s of the predicted pressure points relative to the fitted line but gave more realistic curves. Table 3 summarizes the fitted curves for the predicted rms pressure versus measured rms pressure for both the two-parameter model (columns 3 to 6 of the table) and for the one-parameter model (columns 7 to 9). The second column gives the mean rms pressure \bar{y} for all runs at each location. This was used to normalize the standard deviations relative to the mean in terms of the Coefficient of Variation (COV) given by $COV = 100s/\bar{y}$. As suggested above the best agreement between predicted and measured pressures occurred near the bow. The average slopes of the curves for the one-parameter fit start at about 1.1 at the bow and decrease roughly linearly to about 0.7 near midships (FS 50.75 location) and then remain in the range of 0.75 to 0.90 further aft.

The graphs of rms pressure also show increasing scatter at higher pressure values. The bounds of the scatter roughly form a wedge with an apex at the origin, suggesting that the error band is a constant fraction of the pressure value. The PV-WAVE procedure, POLYFIT, which was used to fit the curves, also provided an error estimate, ϵ , for the standard deviation relative to the fitted curve for each point on the graph. The curves $\epsilon(x)$ were close to linear and it was observed that $\epsilon(x)/x$ was almost constant for each transducer location. A representative value of $\epsilon(x)/x$ for each location is shown in the last column of Table 3. The COV and ϵ/x

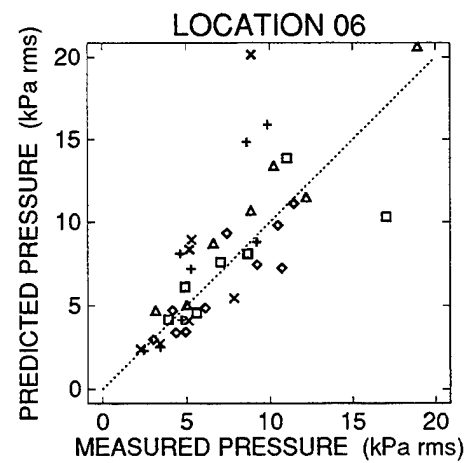
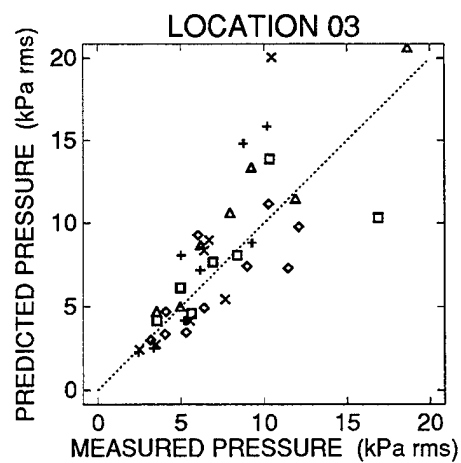
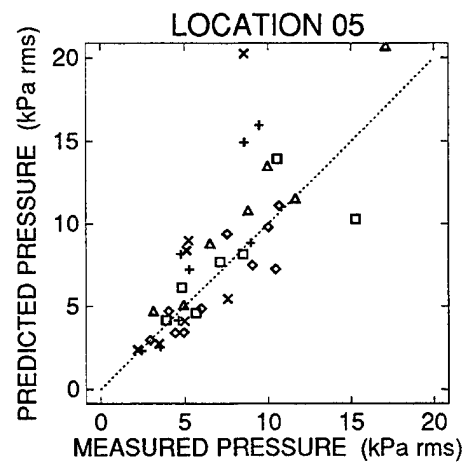
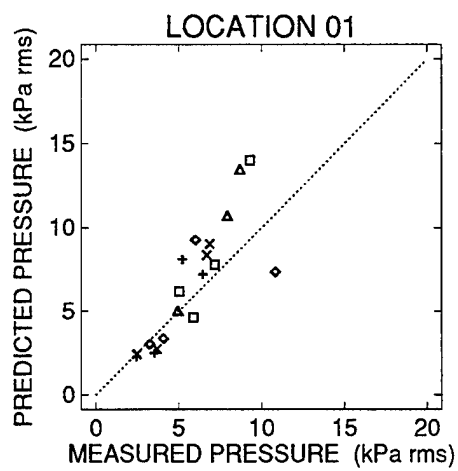


Figure 29: Comparison of the rms hull pressures at frame station 5.25; Dominant Sea: \square Head, \triangle Bow, \diamond Beam, \times Quartering, $+$ Following

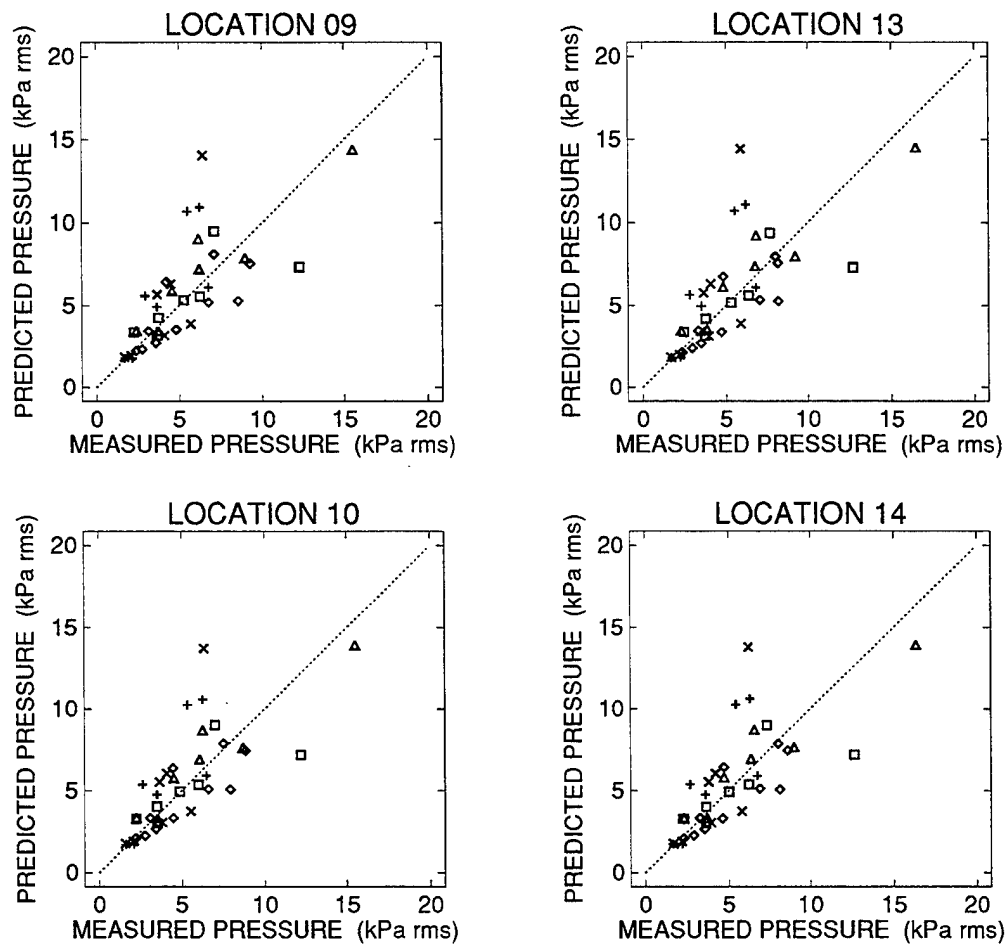


Figure 30: Comparison of the rms hull pressures at frame station 15.25; Dominant Sea: \square Head, \triangle Bow, \diamond Beam, \times Quartering, $+$ Following

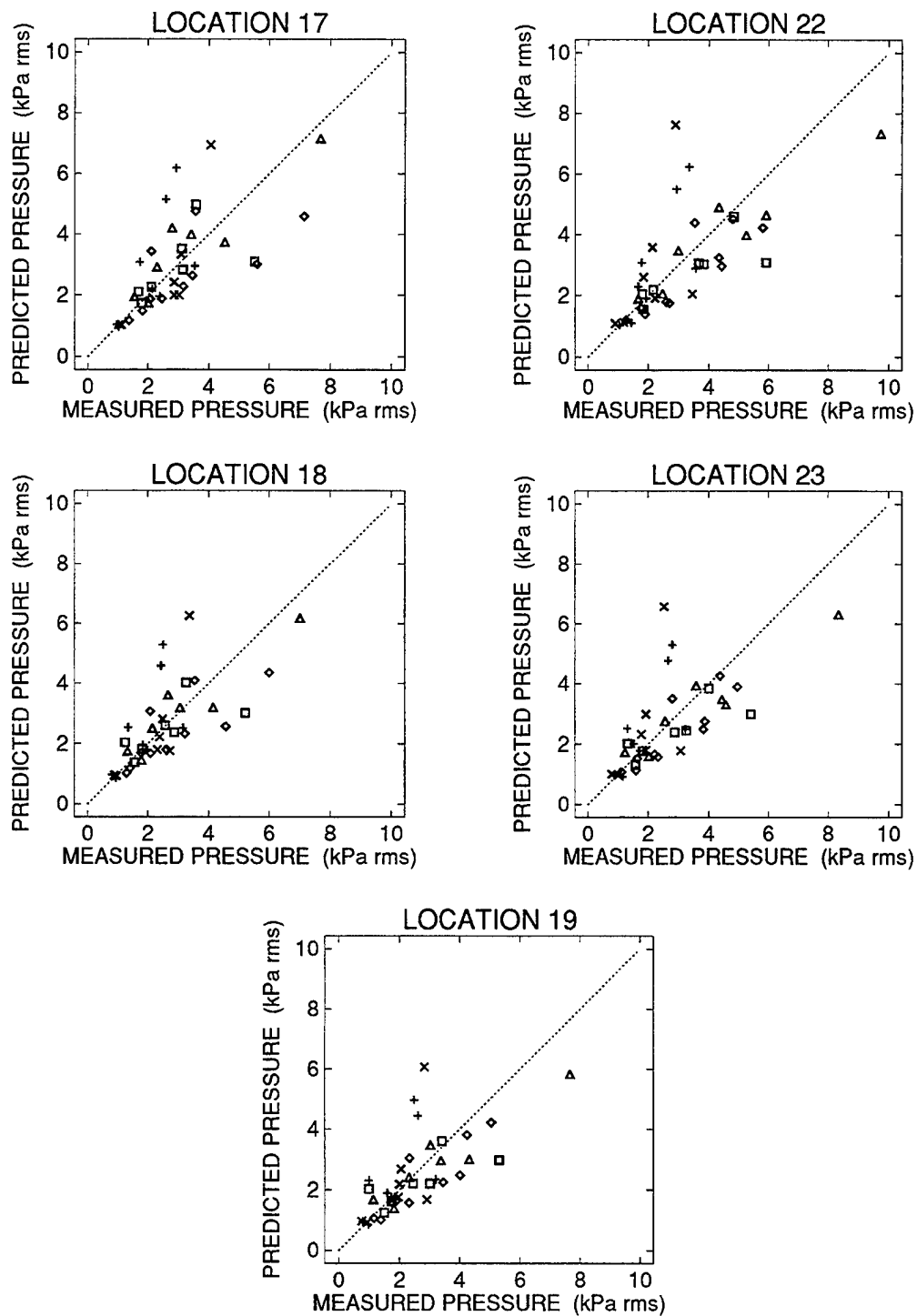


Figure 31: Comparison of the rms hull pressures at frame station 30.75; Dominant Sea: \square Head, \triangle Bow, \diamond Beam, \times Quartering, $+$ Following

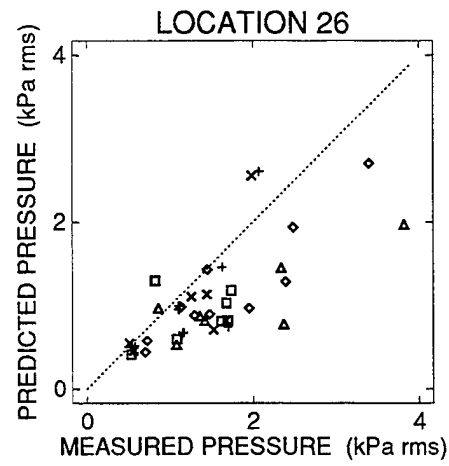


Figure 32: Comparison of the rms hull pressures at frame station 50.75; Dominant Sea: \square Head, \triangle Bow, \diamond Beam, \times Quartering, $+$ Following

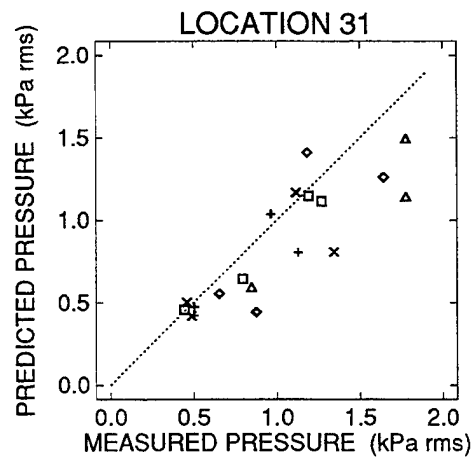


Figure 33: Comparison of the rms hull pressures at frame station 69.5; Dominant Sea: \square Head, \triangle Bow, \diamond Beam, \times Quartering, $+$ Following

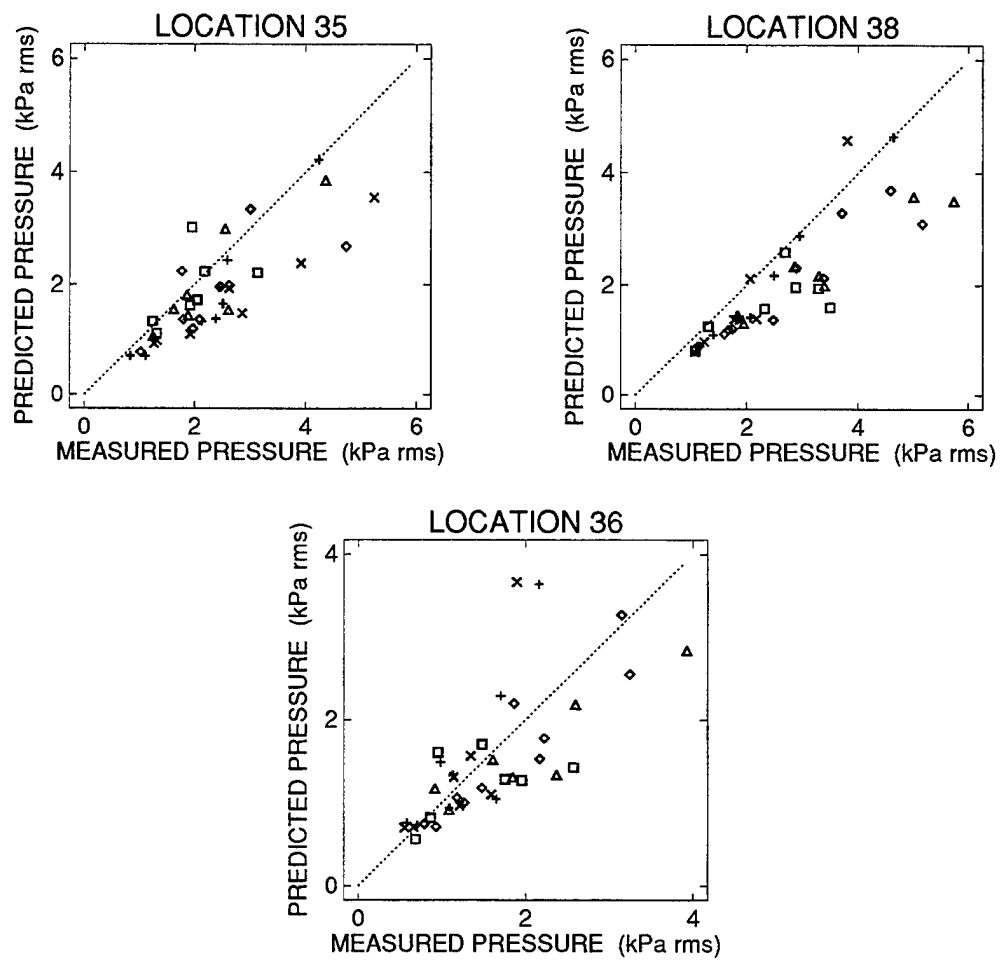


Figure 34: Comparison of the rms hull pressures at frame station 91.75; Dominant Sea: \square Head, \triangle Bow, \diamond Beam, \times Quartering, $+$ Following

Table 3: Linear least squares fit of predicted versus measured hull pressure at each transducer location

Location No.	Mean \bar{y} (kPa)	$y = ax + b$				$y = ax$		
		Intercept b (kPa)	Slope a	Std.Dev. s (kPa)	COV %	Slope a	COV %	Error ϵ/x
FS 5.25								
P1	6.71	-0.81	1.29	2.09	31	1.17	31	0.06
P3	7.93	0.69	0.99	2.90	36	1.07	37	0.05
P5	7.97	0.47	1.07	2.97	37	1.13	37	0.05
P6	7.94	1.05	0.96	3.00	37	1.07	37	0.06
FS 15.25								
P9	5.60	1.44	0.80	2.20	39	1.02	40	0.06
P10	5.41	1.41	0.80	2.09	38	1.01	40	0.06
P13	5.63	1.59	0.77	2.28	40	1.00	42	0.06
P14	5.41	1.49	0.76	2.13	39	0.97	41	0.06
FS 30.75								
P17	2.96	0.94	0.70	1.19	40	0.95	42	0.06
P18	2.57	0.79	0.70	0.99	38	0.94	40	0.06
P19	2.44	0.85	0.64	0.95	38	0.89	42	0.06
P22	3.05	1.02	0.65	1.24	40	0.90	43	0.07
P23	2.62	0.92	0.64	1.05	40	0.89	43	0.07
FS 50.75								
P26	1.06	0.20	0.58	0.41	38	0.69	38	0.06
FS 69.5								
P31	0.84	0.12	0.72	0.19	23	0.82	23	0.05
FS 91.75								
P35	1.92	0.49	0.58	0.55	28	0.74	30	0.05
P36	1.49	0.34	0.73	0.56	37	0.91	38	0.06
P38	1.97	0.09	0.72	0.51	25	0.75	25	0.04

values tend to show highest scatter around frame station FS 30.75 decreasing slightly toward the bow and stern from this location. The graphs for forward frame stations FS 50.75, FS 15.25 and FS 30.75 show five or six runs with nominal following and quartering seas having predicted pressures above the scatter band of the majority of runs. This effect is not evident at stations further aft.

The comparisons of measured and predicted rms hull pressures are plotted based on the dominant wave heading in Figure 35. The results of linear least square curve fitting of these plots are shown in Table 4. The best fit was obtained for bow seas where the predicted rms pressures averaged four percent higher than measured. The head and beam sea predictions averaged 13 and 15 percent lower than measured respectively. For following and quartering seas the predicted rms pressures averaged 34 percent higher than measured. The points on the plots have been identified based on the pressure transducer frame station and show that

Table 4: Linear least squares fit of predicted versus measured hull pressure for each dominant sea direction

Sea Direction	Mean \bar{y} (kPa)	$y = ax + b$				$y = ax$		
		Intercept b (kPa)	Slope a	Std.Dev. s (kPa)	COV %	Slope a	COV %	Error ϵ/x
Head	4.00	0.63	0.78	1.56	39	0.87	40	0.03
Bow	5.33	-0.06	1.05	1.41	26	1.04	26	0.02
Beam	3.56	0.08	0.84	1.06	29	0.85	29	0.02
Quartering	3.82	-1.14	1.58	2.25	58	1.34	60	0.04
Following	4.05	-0.57	1.46	1.59	39	1.34	39	0.03

highest pressures occurred at the forward locations and lowest pressures at the aft locations for all headings. The high slopes of the fitted curves for following and quartering seas are controlled by the over prediction of pressures at forward locations. The points at aft locations are grouped close to the origin for all headings, and for following and quartering seas generally show predicted pressures slightly lower than measured.

6.2.2 Pressure spectra

Graphs comparing predicted and measured hull pressure spectra at 18 transducer locations for each of 39 runs are presented in Appendix C. In many cases there is good agreement between measured and predicted spectra shapes and in other cases significant differences. These differences could be due to differences in the wave spectra as seen by the ship compared to the wave buoy measurement and/or errors in the PRECAL pressure \sqrt{RAO} prediction model. Some of the runs are considered in this section to illustrate various trends and observations. The pressure spectra are plotted as the pressure vs wave frequency normalized to a one Hz bandwidth with units of kPa/\sqrt{Hz} . The pressure power spectral density kPa^2/Hz can be obtained by squaring the pressure spectra values.

Run R7 gave one of the best matches between the predicted and measured pitch spectra for the nominal head seas runs considered in Section 5.1 (see Figure 14). Figure 36 shows a pressure spectrum for one of the hull locations at each frame station for this run. The three forward frame stations all have similar shaped spectra and show good agreement between measurement and prediction. At frame station FS 50.75 the measured spectra have a broader peak than the stations further forward. The predicted spectral shape is roughly correct but 30 to 40 percent lower in amplitude, consistent with the trend of lower rms pressures at this location. Further aft, the predicted spectra show both a different shape and level compared to the measured spectra.

Run R21, also showed good agreement between measured and predicted pitch spectra and, although nominally a head sea run, had a dominant following sea component as discussed in Section 5.1. The spectra for this run, shown in Figure 37, exhibited a much different spectral shape than that for run R7. The spectra contain a fairly narrow low frequency peak which is consistently dominant in all the predicted spectra. The best match with experimental data was at the furthest aft frame station FS 91.75 at locations P35 and P38. The measured peaks for

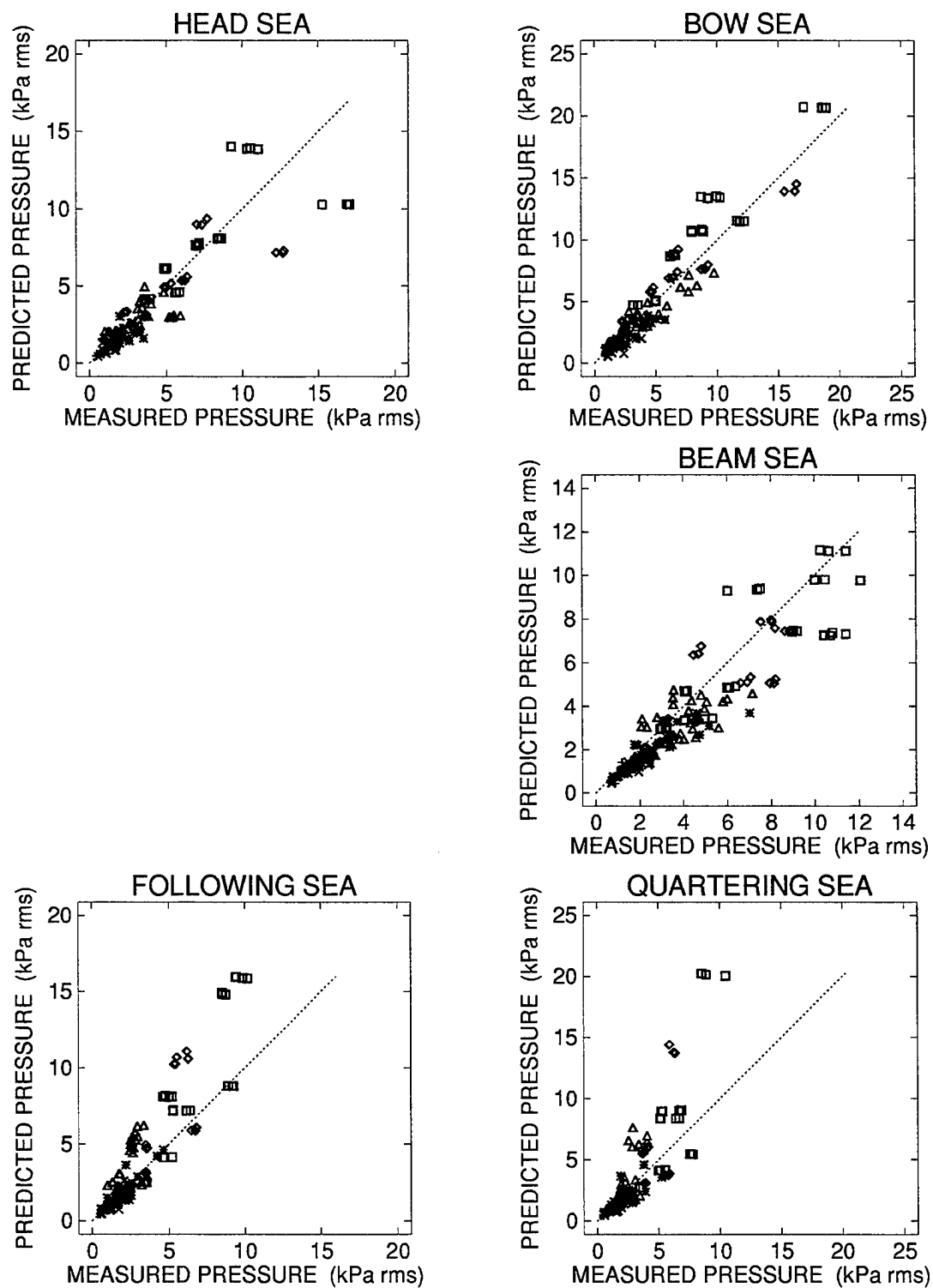


Figure 35: Comparison of the RMS hull pressures sorted by dominant sea direction;
Frame Station: □ 5.25, ◇ 15.25, △ 30.75, × 50.75, + 69.5, * 92.75

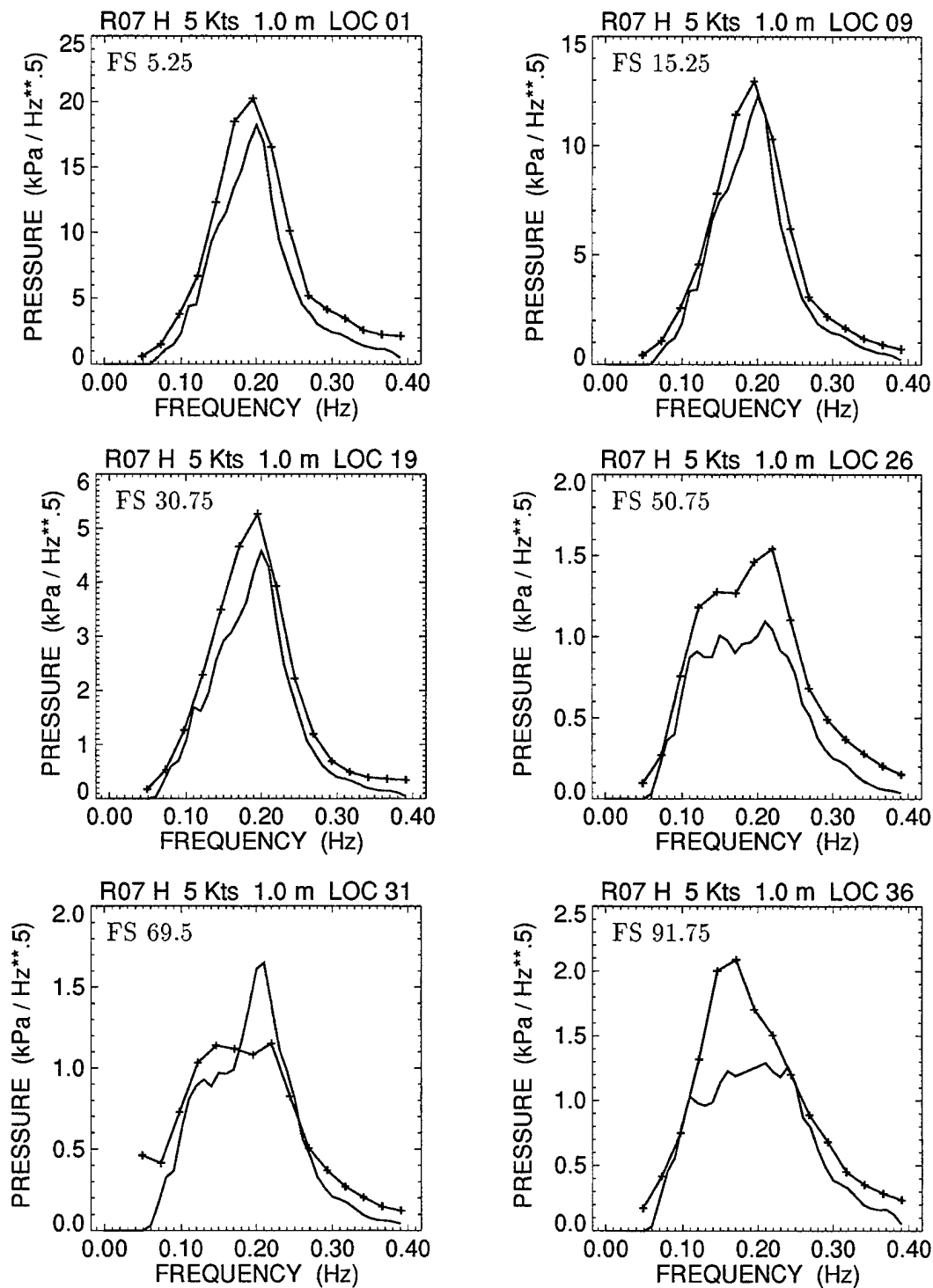


Figure 36: Comparison of hull pressure spectra at different frame stations for Run R7 with dominant head seas; — prediction, + measurement

the keel location P36 at this frame station and at other keel locations were significantly lower than predicted.

Of the beam sea runs considered in Section 5.2, run R31 gave the best agreement between measured and predicted roll angle spectra (refer to Figures 17 and 18). The spectra at several frame stations for this run are shown in Figure 38. There is reasonable agreement at all locations including the prediction of change in spectral shape between bow and stern locations. At frame station FS 31, the spectra are shown for both locations P17 and P22 which are at the same depth but on opposite sides of the ship. For this run the dominant sea was from the starboard beam and the measured pressures were higher on the starboard side of the ship. The PRECAL prediction shows only small differences between the pressures on opposite sides of the ship and at some locations even shows slightly lower pressures on the starboard side. The measured roll angle spectra for the 11 knot beam sea runs, shown in Figure 17, contains a strong peak at 0.08 Hz which was not contained in the PRECAL roll spectra. This is consistent with the differences between the PRECAL and the measured roll $\sqrt{\text{RAOs}}$ in beam seas presented in Figure 20. The pressure spectra for run R5, shown in Figure 39, exhibit closer agreement than the roll spectra for this run and best agreement at locations near the bow and the furthest aft locations. The measured pressure spectra show only a small peak at 0.08 Hz, most noticeable at locations P3 and P38. The predicted spectra show a sharp peak at 0.08 Hz which did not show up at all in the predicted roll spectra.

Figure 40 shows spectra for one of the bow sea runs. For locations near the bow there is good agreement with the exception of the minor peak at 0.07 Hz. The spectra for stations at midship and further aft show lower predicted levels than measured and no longer contain the dominant peak centered at 0.2 Hz which is still present in the measured spectra at the aft locations.

Figure 41 shows spectra for one of the quartering sea runs. Agreement is fairly good at all frame stations. The predicted spectra show a larger peak at 0.07 Hz than found in all of the measured spectra except for location P35 and P38 at the furthest aft frame station where the peaks match well.

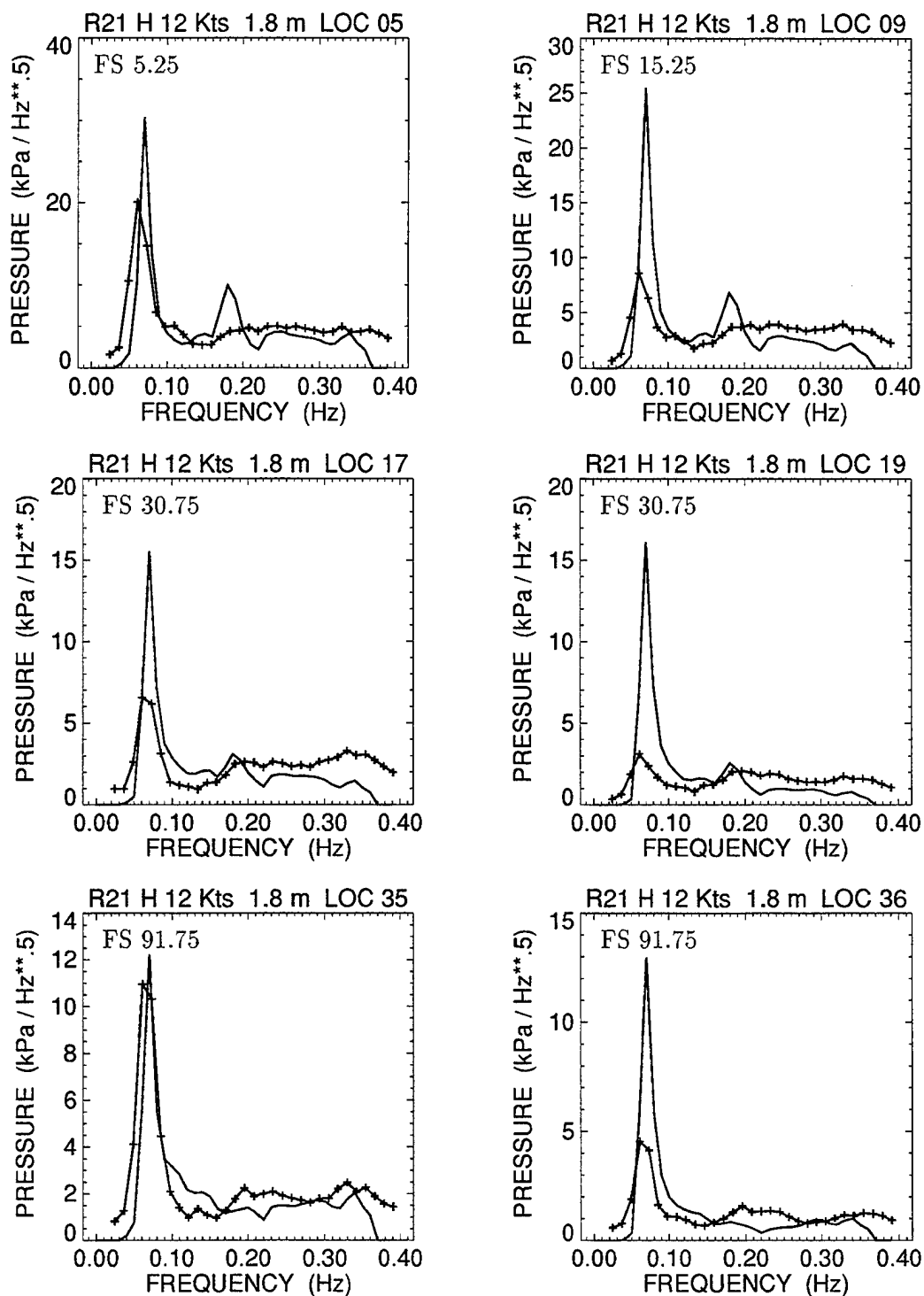


Figure 37: Comparison of hull pressure spectra at different frame stations for Run R21 with dominant following seas; — prediction, + measurement

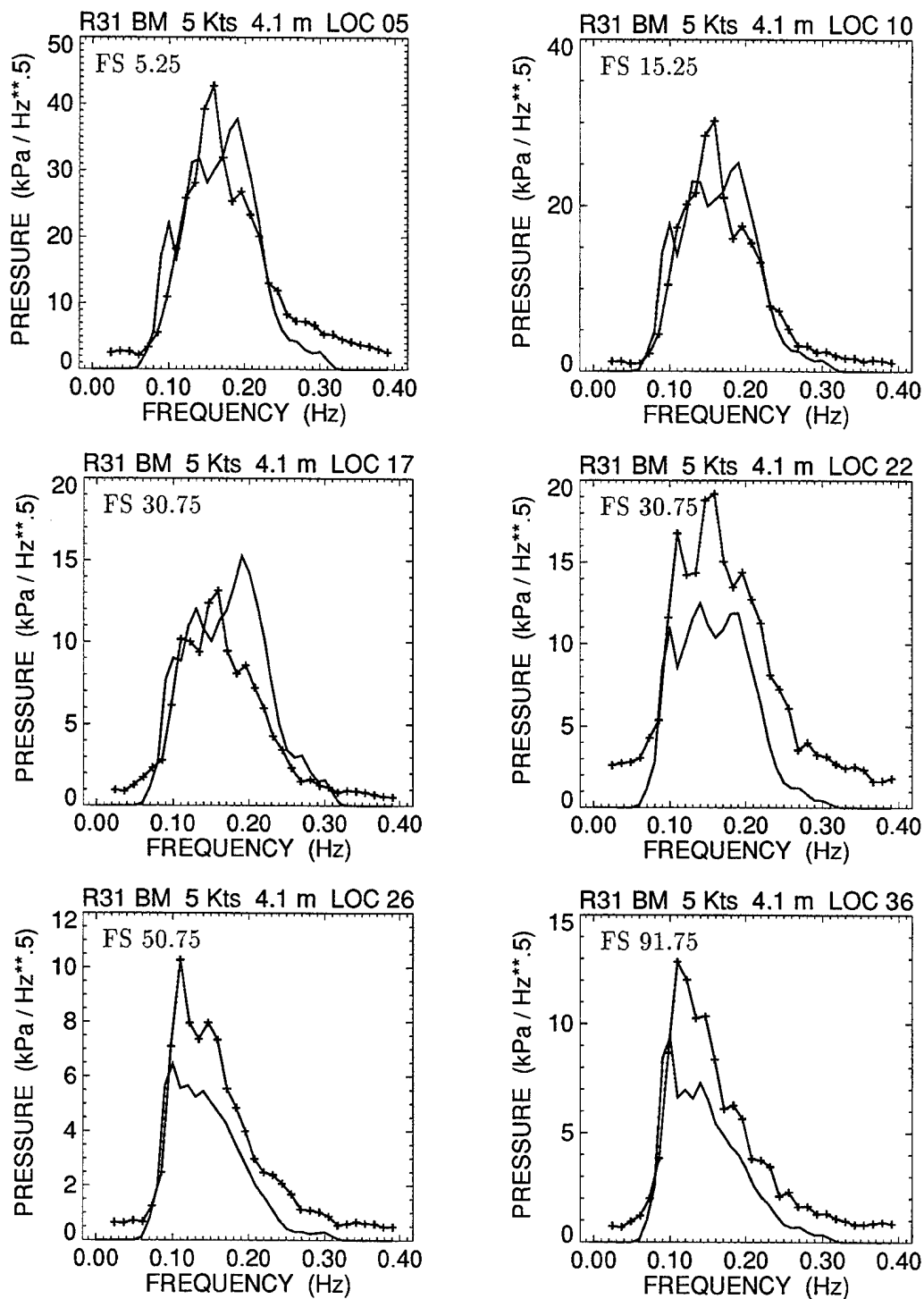


Figure 38: Comparison of hull pressure spectra at different frame stations for Run R31 with dominant beam seas; — prediction, + measurement

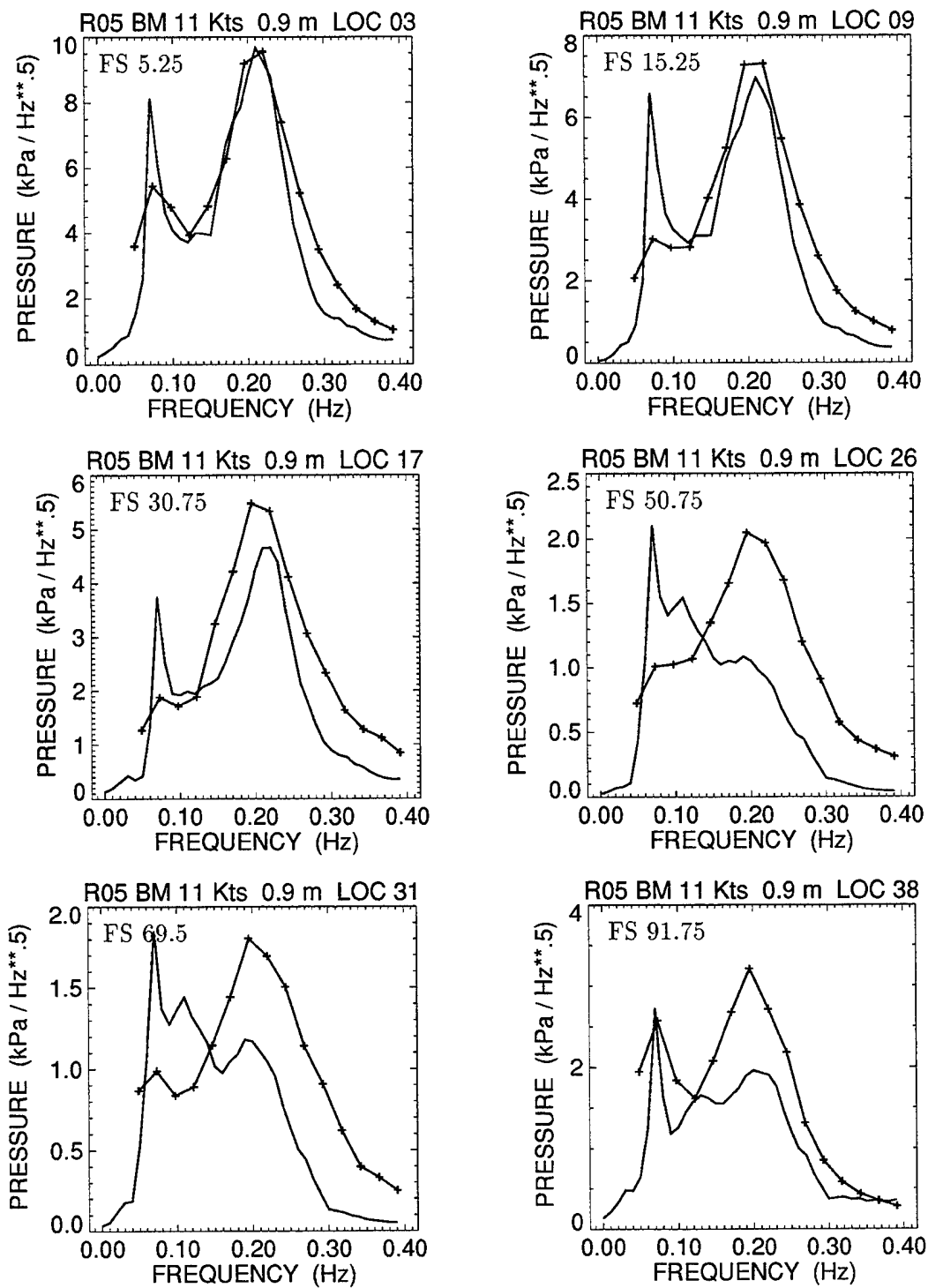


Figure 39: Comparison of hull pressure spectra at different frame stations for Run R5 with dominant beam seas; — prediction, + measurement

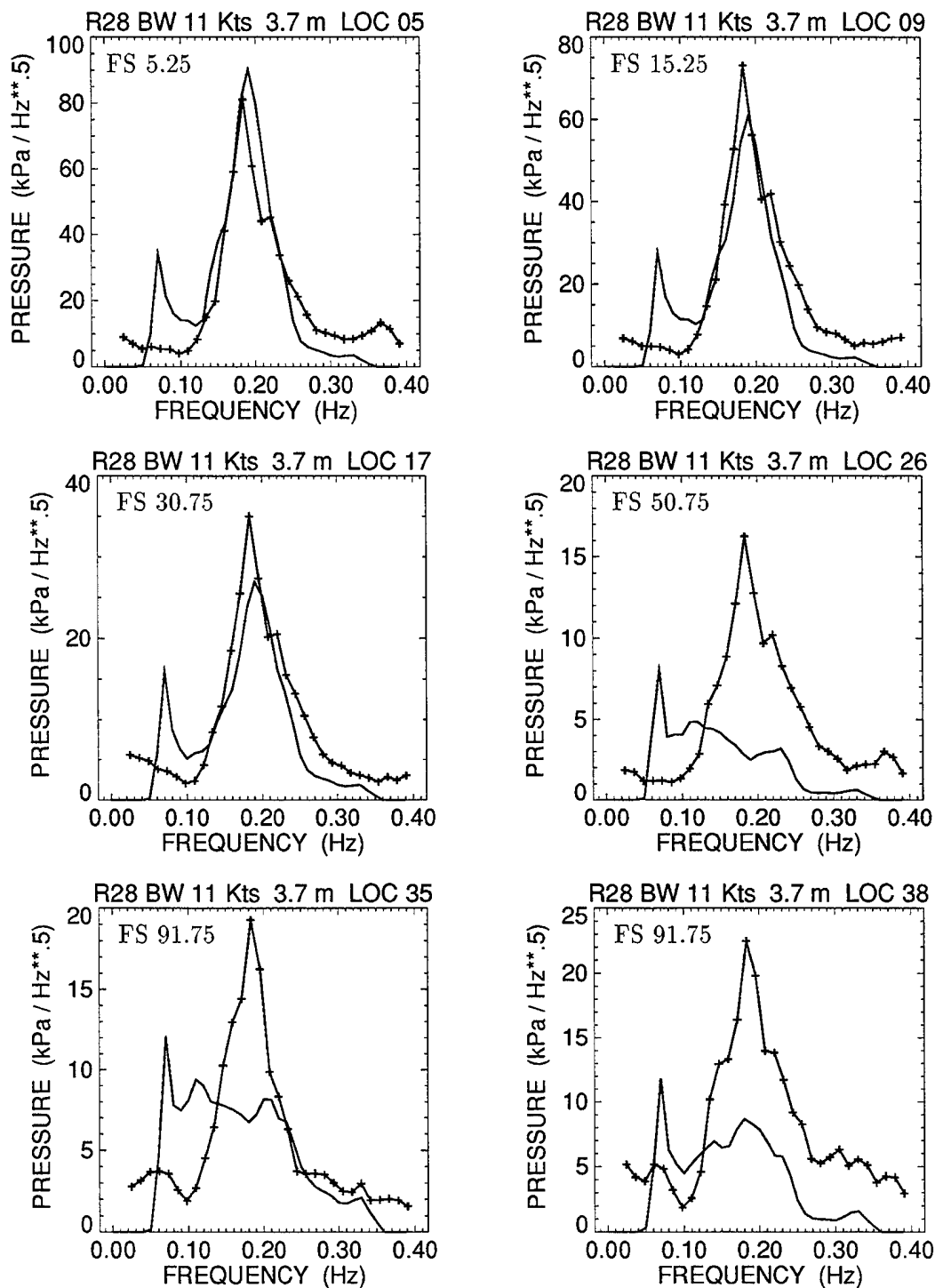


Figure 40: Comparison of hull pressure spectra at different frame stations for Run R28 with dominant bow seas — prediction, + measurement

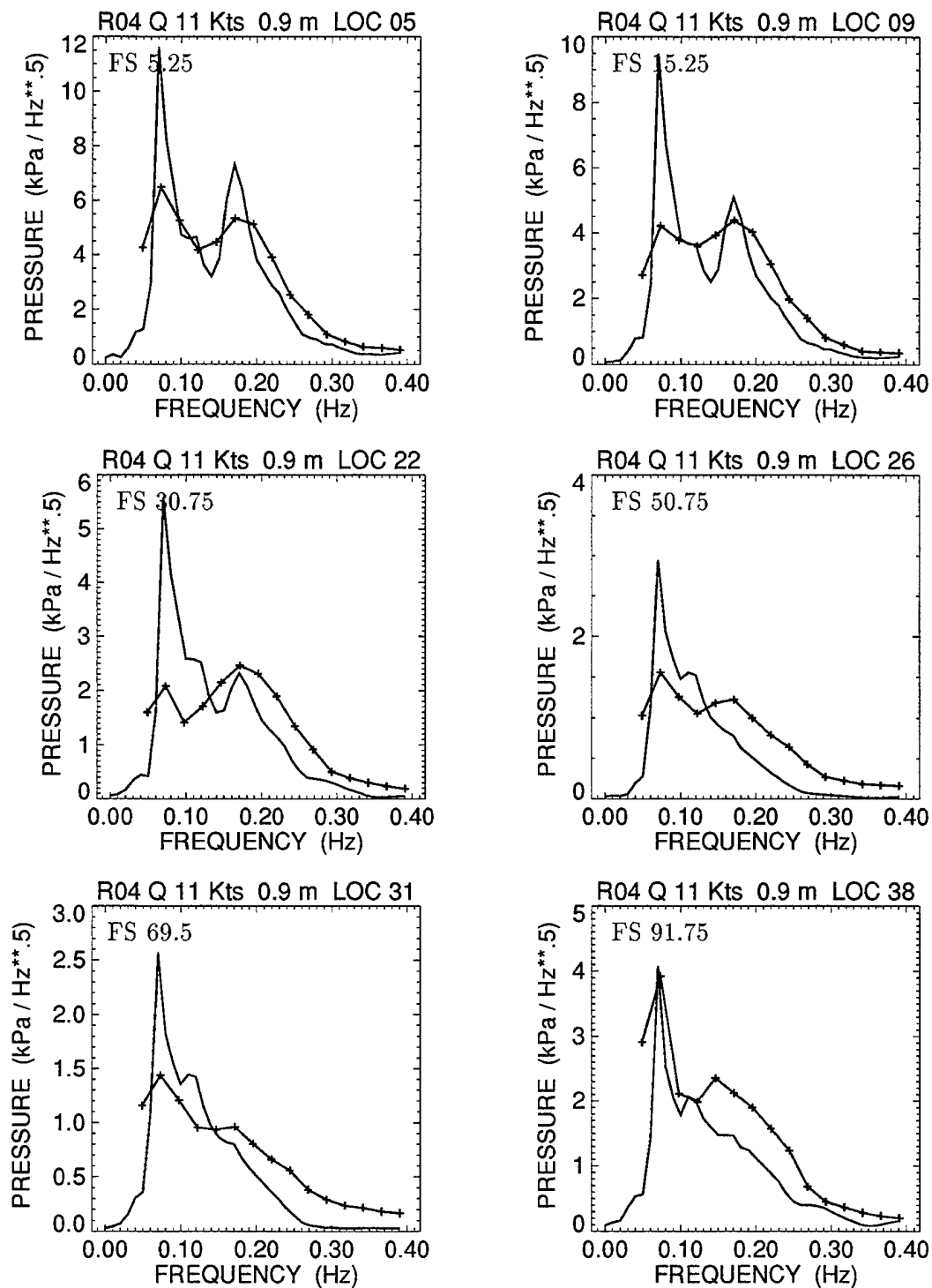


Figure 41: Comparison of hull pressure spectra at different frame stations for Run R4 with dominant quartering seas — prediction, + measurement

7 Summary and Conclusions

Overall, the trial was successful. A fairly good variety of sea states was encountered and data recording equipment functioned well. The small pressure transducers were a disappointment as a significant portion of them failed during the trial or pre-trial testing. Alternatives to this type of transducer were investigated as there had been problems on previous trials but no suitable candidates were found. Further investigation will have to be undertaken before future trials are undertaken. The Labview data acquisition system was programmed to provide a real time data monitoring and analysis capability which was a significant improvement over capabilities in past trials.

In the measurements of the sea state, the directional Endeco Wavetrack wavebuoy proved to be acceptable with the exception of the data for November 11 and possibly November 12 which appeared to have the heading angles in error by 180 degrees. Since it was not possible to characterize the error, the data have been left as measured. This should be kept in mind in the comparison of the measured and predicted spectra where agreement is quite good except that the predicted response has an additional component at a frequency which is not evident in the measured results. Deployment and recovery of the buoy in heavy seas caused some difficulty and resulted in less than ideal sea state measurements on some days. The over-the-bow microwave wave height meter worked well and proved to be very useful for instantaneous sea state estimates in the ship laboratory. The 'MacRadar' system proved useful in ascertaining predominant sea direction in confused seas.

There was good agreement between PRECAL, SHIPMO and trial results for rms pitch motion in head seas. Pitch spectra were in agreement between PRECAL and trial results. There were significant differences in roll $\sqrt{\text{RAOs}}$ between PRECAL, SHIPMO and measured (with and without anti-roll tanks filled) results in beam seas. PRECAL predictions of rms roll were half of the measured roll angle, even with roll tanks in operation (not taken into account in PRECAL prediction). Reducing the roll damping coefficients by half in PRECAL calculations produced good agreement with measured rms roll angles. There were significant differences between predicted and measured roll spectra shape, most noticeable at the higher speeds (11 knots).

In predicting pressure $\sqrt{\text{RAOs}}$, PRECAL irregular frequency suppression worked well at 5 knots. At 11 knots suppression removed many spurious peaks, however, a significant number remained and had to be removed manually. Reducing the roll damping coefficients by half had only a small influence on pressure $\sqrt{\text{RAOs}}$ calculated with PRECAL.

The PRECAL predictions of rms hull pressures showed good agreement with measurements at the bow, averaged 30 percent lower at midships (predictions for only one location on the keel) and averaged 10 to 25 percent lower at stations further aft. PRECAL predictions of pressure spectra gave good agreement with measured results at the bow for many of the runs, but poorer agreement in spectral shape at midships and further aft. A few runs showed poorer agreement in spectral shape at all locations, suggesting differences between the wave spectra seen by the ship during the run and the directional wave spectra measured by the wavebuoy.

Considering the number of uncertainties and sources of error in full scale trials, the comparison of predicted and measured ship motions and hull pressures was satisfactory. The most significant result in considering structural performance is the ability to predict strains in the hull structure resulting from the sea state. This part of the problem is being addressed in a

follow-on report.

Acknowledgments

The authors would like to thank Lt. Craig Evans for assisting with data analysis and carrying out the initial PRECAL runs, Sam Ando for providing advice on running PRECAL and constructing the Quest PRECAL model, and Kevin McTaggart for conducting ship motion analyses of QUEST with SHIPMO.

References

- [1] "NSMB CRS PRECAL Working Group User's Manual, Motion, Load, and Pressure Program Suite - PRECAL", BMT SeaTech CRS Report, January, 1995.
- [2] "MacRadar, Wavetrack, and Natwav Spectra from QUEST Cruise Q210", MacLaren Plansearch (1991) Limited, DREA Contractor Report CR/94/421, April 1991.
- [3] PV-WAVE Command Language Reference, Precision Visuals Inc., Boulder Colorado, 1992
- [4] McTaggart, K.A., "SHIPMO6 an Updated Strip Theory Ship Motion Program", DREA Technical Memorandum 93/213, October 1993.
- [5] Miles, M., "Tuning and Evaluation of Anti-Roll Tanks on CFAV QUEST", NRC, Division of Mechanical Engineering, Marine Dynamics and Ship Laboratory, Report No. LTR-SH-122, January 1972.

Appendix

The Appendices for this report are contained in a separate Volume II.

UNCLASSIFIED

SECURITY CLASSIFICATION OF FORM
(highest classification of Title, Abstract, Keywords)

DOCUMENT CONTROL DATA <small>(Security classification of title, body of abstract and indexing annotation must be entered when the overall document is classified)</small>		
1. ORIGINATOR (The name and address of the organization preparing the document. Organizations for whom the document was prepared, e.g. Establishment sponsoring a contractor's report, or tasking agency, are entered in section 8.) Defence Research Establishment Atlantic P.O. Box 1012, Dartmouth, N.S. B2Y 3Z7	2. SECURITY CLASSIFICATION <small>(Overall security of the document including special warning terms if applicable.)</small> <p style="text-align: center; font-size: 1.2em;">Unclassified</p>	
3. TITLE (The complete document title as indicated on the title page. Its classification should be indicated by the appropriate abbreviation (S,C,R or U) in parentheses after the title.) <p style="text-align: center; font-size: 1.2em;">Measurement and Linear Prediction of Hull Pressure Spectra on CFAV QUEST - Results of Q210 — Volume I</p>		
4. AUTHORS (Last name, first name, middle initial. If military, show rank, e.g. Doe, Maj. John E.) <p style="text-align: center;">STREDULINSKY, David C., PEGG, Neil G., and GILROY, Layton E.</p>		
5. DATE OF PUBLICATION (Month and year of publication of document.) <p style="text-align: center;">July 1996</p>	6a. NO. OF PAGES (Total containing information. Include Annexes, Appendices, etc.) <p style="text-align: center;">Volume I - 59 Volume II - 232</p>	6b. NO. OF REFS. (Total cited in document.) <p style="text-align: center;">5 / 0</p>
6. DESCRIPTIVE NOTES (The category of the document, e.g. technical report, technical note or memorandum. If appropriate, enter the type of report, e.g. interim, progress, summary, annual or final. Give the inclusive dates when a specific reporting period is covered.) <p style="text-align: center;">DREA Technical Memorandum</p>		
8. SPONSORING ACTIVITY (The name of the department project office or laboratory sponsoring the research and development. include the address.) Defence Research Establishment Atlantic P.O. Box 1012, Dartmouth, N.S. B2Y 3Z7		
9a. PROJECT OR GRANT NUMBER (If appropriate, the applicable research and development project or grant number under which the document was written. Please specify whether project or grant.) <p style="text-align: center;">1.g.e</p>	9b. CONTRACT NUMBER (If appropriate, the applicable number under which the document was written.) 	
10a. ORIGINATOR'S DOCUMENT NUMBER (The official document number by which the document is identified by the originating activity. This number must be unique to this document.) <p style="text-align: center;">DREA Technical Memorandum 96/229 Volume I</p>	10b. OTHER DOCUMENT NUMBERS (Any other numbers which may be assigned this document either by the originator or by the sponsor.) 	
11. DOCUMENT AVAILABILITY (Any limitations on further dissemination of the document, other than those imposed by security classification) <div style="margin-left: 20px;"> <input checked="" type="checkbox"/> Unlimited distribution <input type="checkbox"/> Distribution limited to defence departments and defence contractors; further distribution only as approved <input type="checkbox"/> Distribution limited to defence departments and Canadian defence contractors; further distribution only as approved <input type="checkbox"/> Distribution limited to government departments and agencies; further distribution only as approved <input type="checkbox"/> Distribution limited to defence departments; further distribution only as approved <input type="checkbox"/> Other (please specify): </div>		
12. DOCUMENT ANNOUNCEMENT (Any limitation to the bibliographic announcement of this document. This will normally correspond to the Document Availability (11). However, where further distribution (beyond the audience specified in 11) is possible, a wider announcement audience may be selected.) <p style="text-align: center;">Unlimited Distribution</p>		

UNCLASSIFIED

SECURITY CLASSIFICATION OF FORM

DCDO3 2/06/87

UNCLASSIFIED
SECURITY CLASSIFICATION OF FORM

13. **ABSTRACT** (a brief and factual summary of the document. It may also appear elsewhere in the body of the document itself. It is highly desirable that the abstract of classified documents be unclassified. Each paragraph of the abstract shall begin with an indication of the security classification of the information in the paragraph (unless the document itself is unclassified) represented as (S), (C), (R), or (U). It is not necessary to include here abstracts in both official languages unless the text is bilingual).

Trial Q210 was undertaken in November 1993 on CFAV QUEST to measure hull pressure loads and structural response during various operational conditions in moderate seas. This memorandum describes results of measurements and predictions for ship motions and for the pressure loads; results for the strain measurements and predictions will be discussed in a later report. Pressure spectra derived from the measurements are compared to predictions from PRECAL, a three-dimensional linear ship motion and load prediction code. The measured and predicted pressure spectra show reasonable agreement, indicating the strong potential of using PRECAL to predict fatigue load histories for ship hull structures.

This report is presented in two volumes with Volume I containing the main body and Volume II containing the Appendices. Volume I will be given full distribution with Volume II being distributed only on request.

14. **KEYWORDS, DESCRIPTORS or IDENTIFIERS** (technically meaningful terms or short phrases that characterize a document and could be helpful in cataloguing the document. They should be selected so that no security classification is required. Identifiers, such as equipment model designation, trade name, military project code name, geographic location may also be included. If possible keywords should be selected from a published thesaurus. e.g. Thesaurus of Engineering and Scientific Terms (TEST) and that thesaurus-identified. If it not possible to select indexing terms which are Unclassified, the classification of each should be indicated as with the title).

ship motion
hull pressure
ocean wave spectra
wavebuoys

UNCLASSIFIED
SECURITY CLASSIFICATION OF FORM